



SoftCOM '17

tutorials

**Human Safety and Medical
Application of Electromagnetic
Fields: Role of Computational
Modeling**

by

Akimasa Hirata

Nagoya Institute of Technology, Japan

September 21 - 23, 2017.



HUMAN SAFETY AND MEDICAL APPLICATION OF ELECTROMAGNETIC FIELDS: ROLE OF COMPUTATIONAL MODELING

Akimasa Hirata

Nagoya Institute of Technology, Japan

1. International Standardization Activity for Human Safety

References

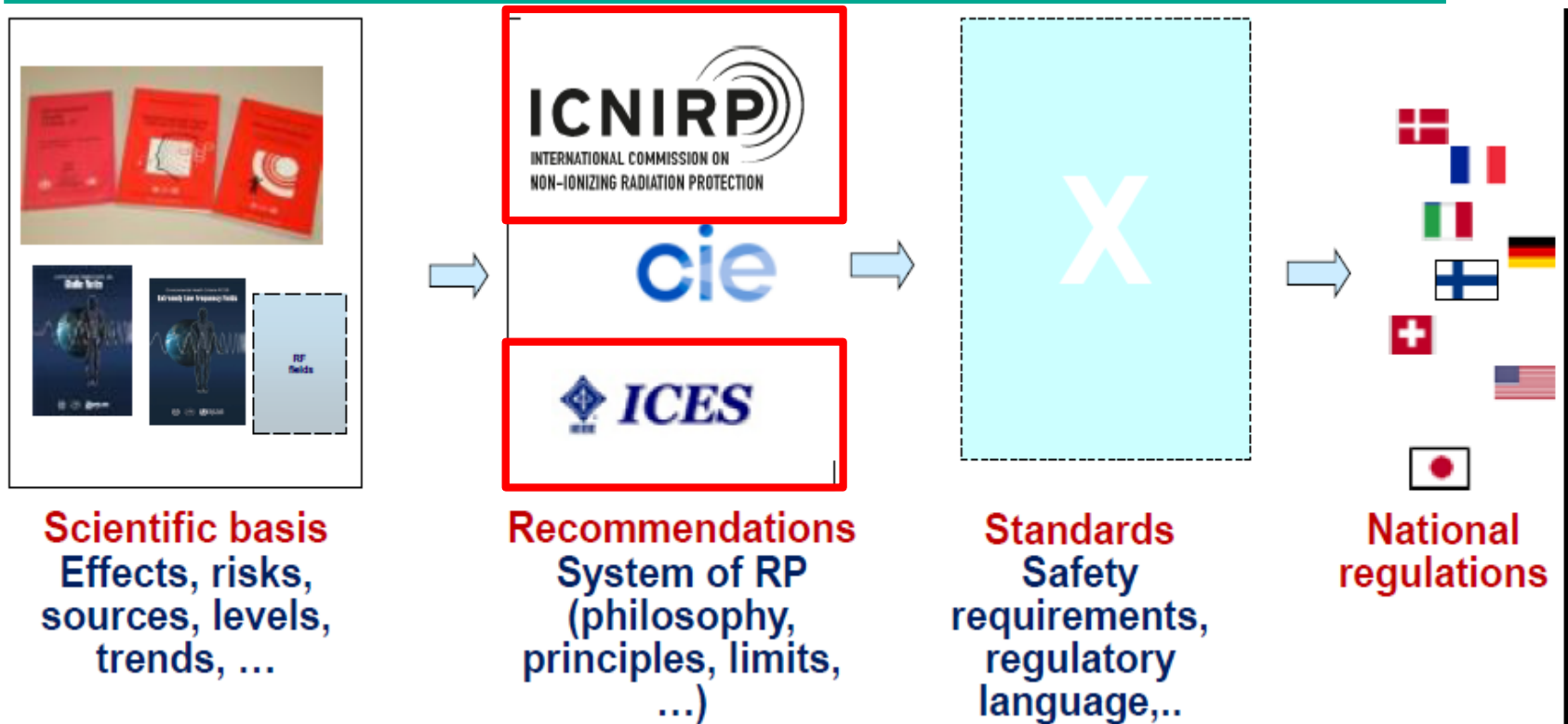
ICNIRP (International Commission on Non-Ionizing Radiation Protection)
<http://www.icnirp.org/>

IEEE International Committee on Electromagnetic Safety (ICES)
<http://www.ices-emfsafety.org/>

LANDSCAPE OF WHO

SLIDE OF DR. VAN DEVENTER (ICNIRP WORKSHOP MAY 2016)

<http://www.icnirp.org/en/workshops/article/workshop-nir2016.html>

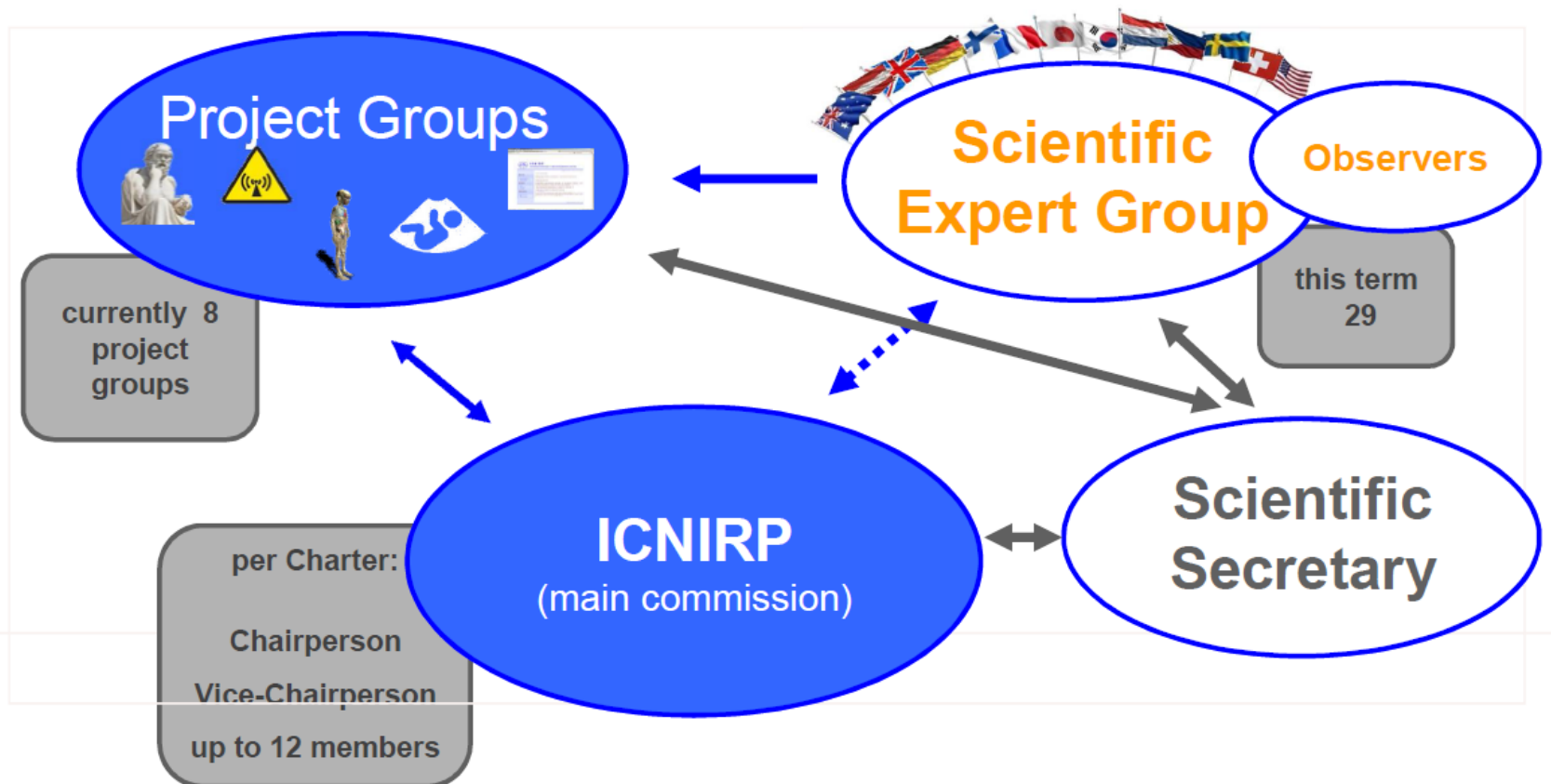


These two international guidelines/standard are based on almost identical health effects. The limit prescribed in these two standard tend to be harmonized gradually.

ICNIRP STRUCTURE (1)

(FROM R. MATTHES SLIDE AT WORKSHOP MAY 2016)

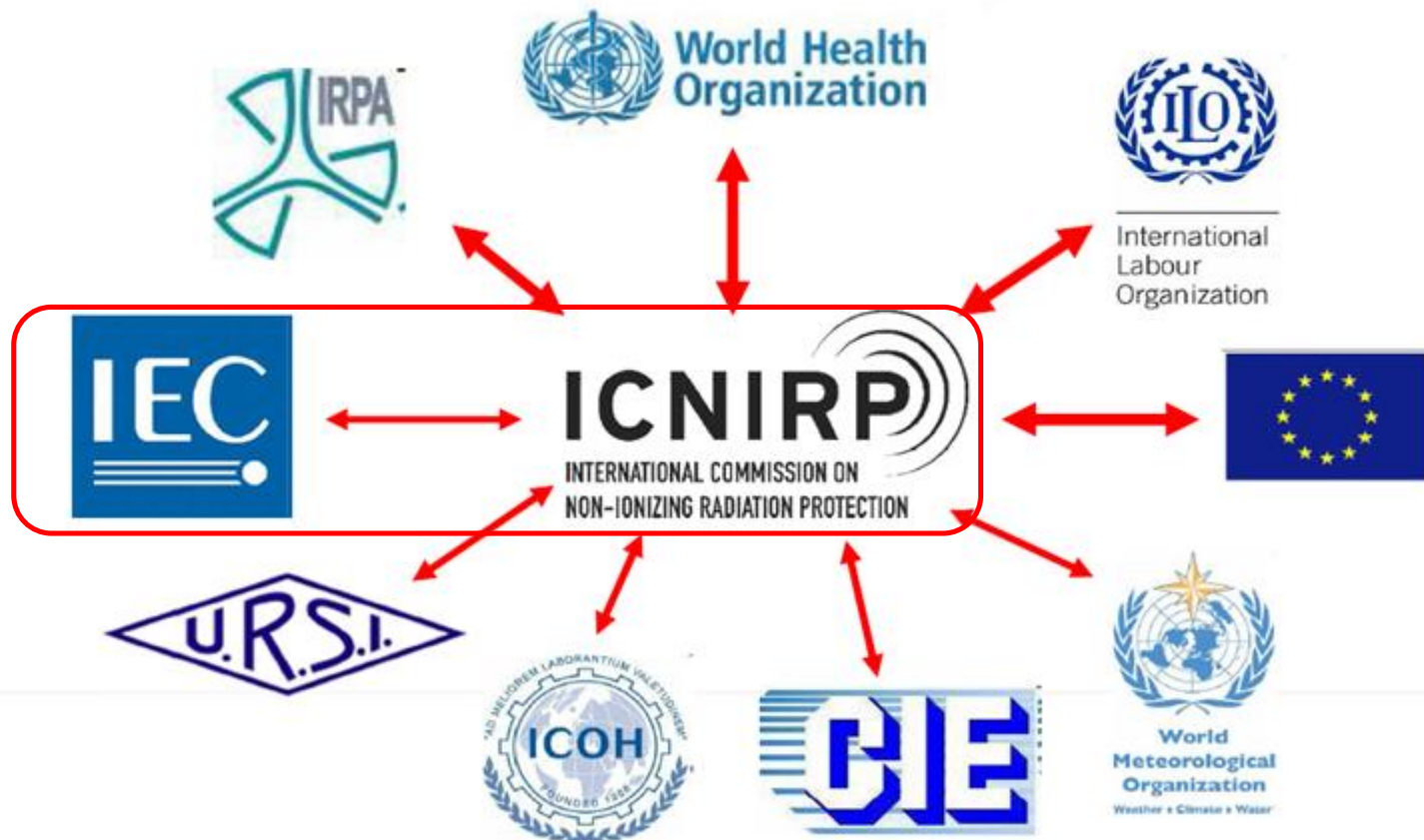
Current structure



A. Hirata is one of 12 members

ICNIRP STRUCTURE (2)

(FROM R. MATTHES SLIDE AT WORKSHOP MAY 2016)



INTERNATIONAL COMMITTEE ON ELECTROMAGNETIC SAFETY (ICES)

“Development of standards for the **safe use of electromagnetic energy** in the range of 0 Hz to 300 GHz relative to the potential hazards of exposure of humans, volatile materials, and explosive devices to such energy. Such standards will be **based on established adverse health effects** and will include safety levels for human exposure to electric, magnetic and electromagnetic fields, including induced currents from such fields, methods for the assessment of human exposure to such fields, standards for products that emit electromagnetic energy by design or as a by-product of their operation, and environmental limits.”

IEEE EXPOSURE STANDARDS HISTORY

1960: USASI C95 Radiation Hazards Project and Committee chartered

1966: USAS C95.1-1966

- 10 mW/cm² (10 MHz to 100 GHz)
- based on simple thermal model

1974: ANSI C95.1-1974 (limits for E² and H²)

1982: ANSI C95.1-1982 (incorporates dosimetry SAR)

1991: IEEE C95.1-1991 (two tiers – reaffirmed 1997)

2002: IEEE C95.6-2002 (0-3 kHz)

2006: IEEE C95.1-2005 (3 kHz -300 GHz) published on April 19, 2006
(comprehensive revision, 250 pages, 1143 ref.)

2014: IEEE C95.1-2345-2014 (0 Hz to 300 GHz) published on May 30, 2014
(NATO/IEEE agreement)

TC95 ACTIVITY

SC-6 (EMF Dosimetry Modeling)

- The goal of SC 6 will be the eventual resolution of uncertainties, and **recommendation of analysis tools/data applicable to human exposure standards**, in addition **to follow and assess the recent literature on EMF dosimetry modeling** both for nerve stimulation effects caused by EMF at frequencies below ~100 kHz and for heating effects caused by RF energy absorption at frequencies above ~100 kHz.
- SC-6 will coordinate closely with the other subcommittees, especially with SC 3 and SC 4, who are currently working on the update and merger of IEEE Std C95.1&C95.6 into a single standard.

DIFFERENCE BETWEEN LF AND RF

	LF	RF	
Adverse Effect	Pain/ Sensory Effect	Thermal Effect	Human safety
Additional modeling is needed to explain measured phenomena	Nerve Activation (e.g., SENN)	Temperature Elevation	
Metric in standards; electromagnetic modeling	In-situ electric field	SAR	Product safety
Dosimetry modeling	Multi-scale simulation	Multi-physics simulation	

WGs IN SC6

- **WG1: “Resolving uncertainties related to electrostimulation threshold in the ELF range”** (A. Legros and I. Laakso)

SCOPE: Resolve uncertainties related to measured and computed thresholds for electrostimulation in the context of exposure to external ELF electromagnetic fields

- **WG2: “Numerical Artifacts”** (Chaired by D. Poljak and K. Yamazaki; Secretary: M. Cvekovic)

SCOPE: Study and quantify effects of numerical artifacts in low frequency (LF) dosimetry; two papers have been published in IEEE T-EMC.

- **WG3: “Intercomparison”** (Chaired by G. Schmid)

SCOPE: Study and quantify effects of numerical artifacts in low frequency (LF) dosimetry

RESEARCH AGENDA BY IEEE ICES

IOP Publishing | Institute of Physics and Engineering in Medicine

Physics in Medicine & Biology

Phys. Med. Biol. 61 (2016) R138–R149

doi:10.1088/0031-9155/61/12/R138

Low-frequency electrical dosimetry: research agenda of the IEEE International Committee on Electromagnetic Safety

J Patrick Reilly¹ and Akimasa Hirata²

¹ Metatec Associates, 12516 Davan Drive, Silver Spring, MD 20904, USA

² Department of Computer Science and Engineering, Nagoya Institute of Technology,
Showa-ku, Gokiso-cho, Nagoya 466–8555, Japan

E-mail: jpreilly@ieee.org and ahirata@nitech.ac.jp

Received 11 November 2015, revised 26 January 2016

Accepted for publication 4 February 2016

Published 25 May 2016



CrossMark

<http://iopscience.iop.org/article/10.1088/0031-9155/61/12/R138/meta>

2. Techniques of Computational Dosimetry

References:

Human Body Models

http://emc.nict.go.jp/bio/model/model01_1_e.html

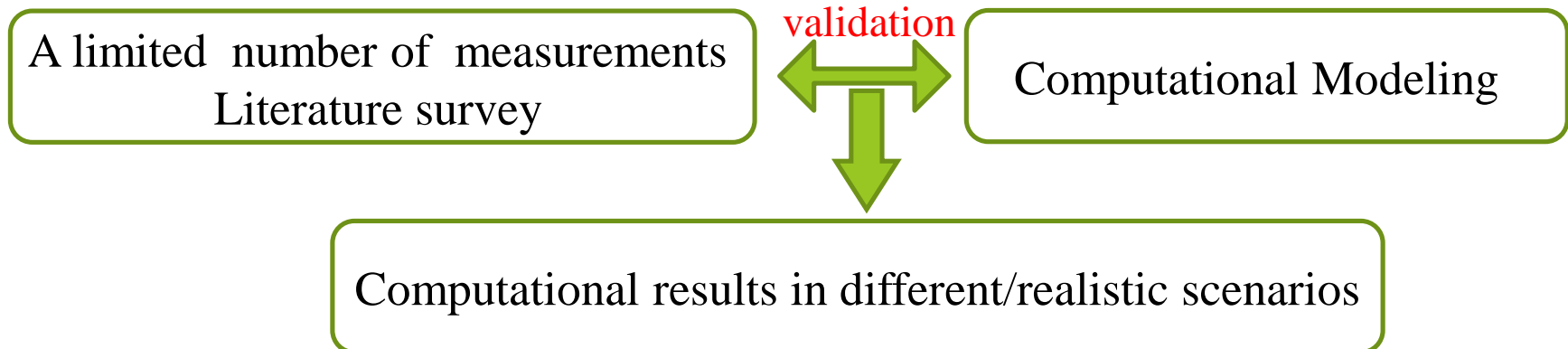
<https://www.itis.ethz.ch/virtual-population/virtual-population/overview/>

Also see the IEEE ICES Research Agenda for LF dosimetry

<http://iopscience.iop.org/article/10.1088/0031-9155/61/12/R138/meta>

DOSIMETRY: ROLE AND VALIDATION (HF)

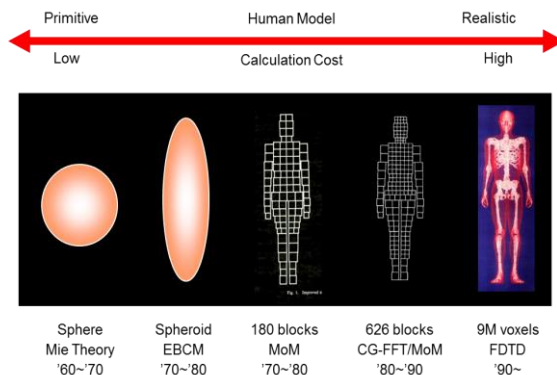
- It is unrealistic to conduct many measurements for excessive heat load due to ethical reasons.
- We can simulate temperature elevation for ambient heat and microwaves **after computational methods are validated**.
- Multi-physics modeling: Electromagnetics and thermodynamics (considering **core temperature change**) in anatomically based model (50+ tissues)
- Plus the thermoregulatory response (vasodilation, sweating)



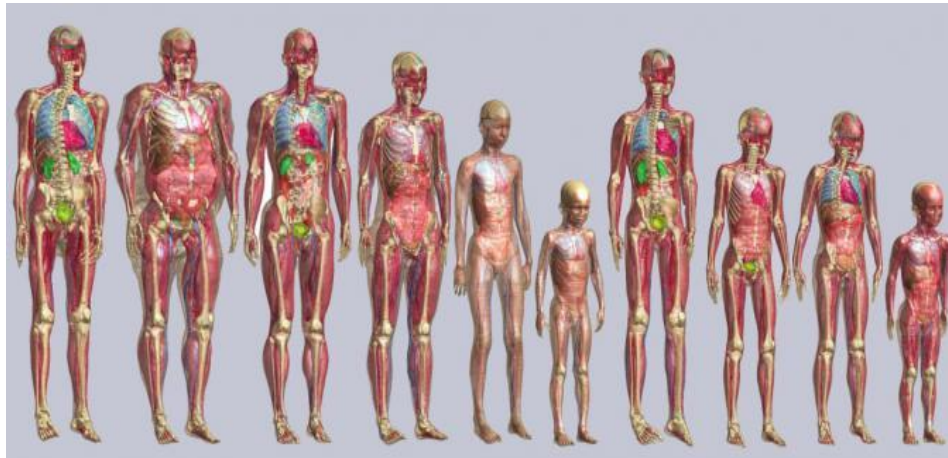
HUMAN MODELING IN HF REGION

Analytical or **numerical human models** have been used to evaluate induced physical quantity. For experimental ones, **physical human phantoms** have been used.

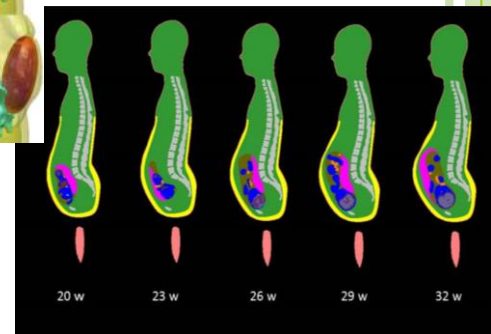
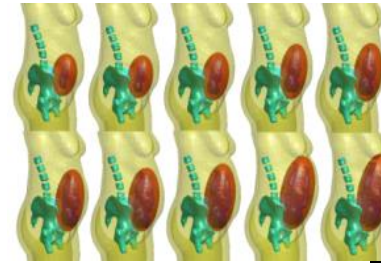
- **Numerical human models** are one of the most important advances in the dosimetry, which have fine spatial resolutions with accurate anatomical structure based on CT and MRI technology.
- **Physical human phantoms** have relatively **poor anatomical structure**, frequently consist of **single material** such as tissue-equivalent liquid. Physical human phantoms have widely been used in **the compliance evaluations of radio devices** because actual radio devices can be used for the evaluation and the simple phantom can provide highly-reproducible and worst-side evaluation.



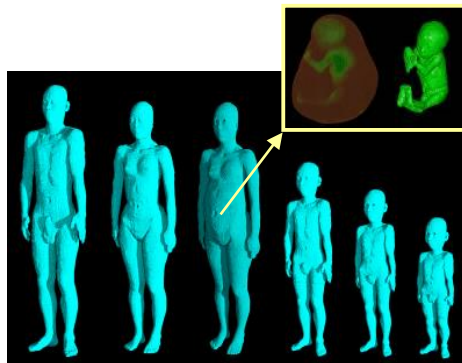
LATEST NUMERICAL HUMAN MODELS



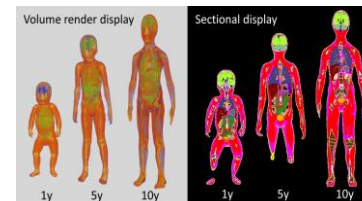
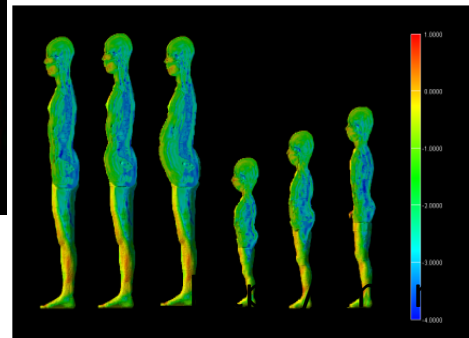
From the homepage of IT'IS foundation.



France-Japan research project (FETUS)



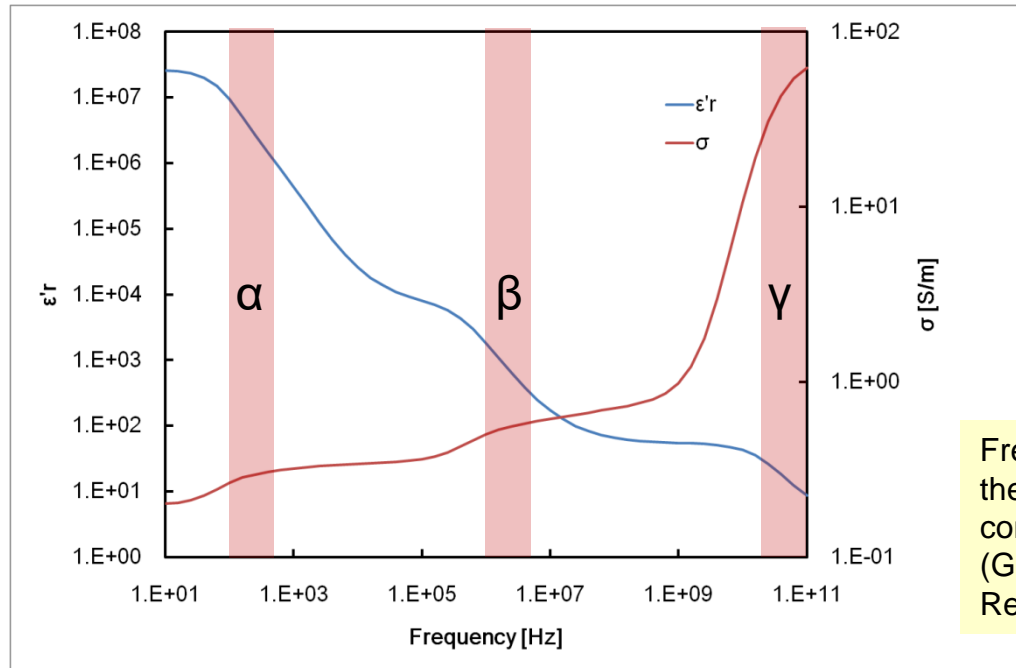
NICT's voxel human models.



	Developed models		ICRP ref. data		% Diff. from ICRP ref. data	
	Height (cm)	Weight (kg)	Height (cm)	Weight (kg)	Height	Weight
1y	76.0	9.4	76.0	10.0	0.0	6.21
5y	109.0	18.8	109.0	19.0	0.0	0.92
10y	138.0	32.2	138.0	32.0	0.0	0.69

http://www.nict.go.jp/bio/model/model01_1_e.html

ELECTRICAL PROPERTIES OF BIOLOGICAL TISSUES AND ORGANS (1)

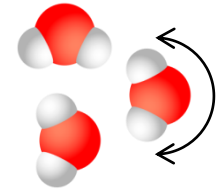
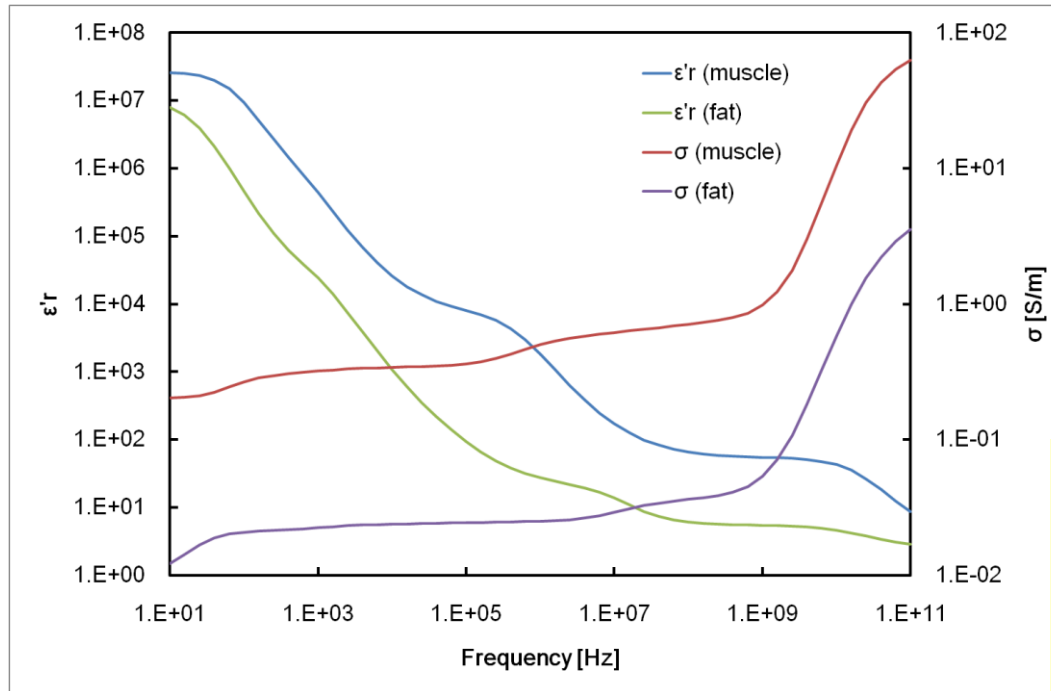


Frequency characteristics of the relative permittivity and conductivity of muscle tissue (Gabriel, et al., Brooks AFB Report, 1996).

Biological tissues and organs are **lossy dielectric**, which is characterized with the relative permittivity (ϵ'_r) and conductivity (σ) or with the relative complex permittivity ($\epsilon'_r - j \epsilon''_r$).

Three relaxations, known as **α , β , and γ dispersion**, appear in the frequency characteristics of the electrical properties of the biological tissues or organs.

ELECTRICAL PROPERTIES OF BIOLOGICAL TISSUES AND ORGANS (2)



Rotation of water molecules[†] causes γ dispersion.

Frequency characteristics of the relative permittivity and conductivity of muscle as a high-water-content tissue and fat as a low-water-content one (Gabriel, et al., Brooks AFB Report, 1996).

Electrical properties of biological tissues and organs are significantly variable, which can be 100 times.

Electrical properties, especially conductivity, strongly depend on the **water-content ratio** of the biological tissues or organs.

(†) http://commons.wikimedia.org/wiki/File:Water_molecule.svg

TEMPERATURE COMPUTATION: CONVENTIONAL EQUATIONS FOR TEMPERATURE RISES

◆ Bio-heat Equation

$$C(\vec{r}) \cdot \rho(\vec{r}) \frac{\partial T(\vec{r}, t)}{\partial t} = \nabla \cdot (K(\vec{r}) \nabla T) + A(\mathbf{r}) + \rho(\vec{r}) \cdot SAR(\vec{r}) - B(\mathbf{r}) \cdot (T(\vec{r}, t) - T_b)$$

◆ Boundary condition

$$-K(\vec{r}) \frac{\partial T(\vec{r}, t)}{\partial n} \Big|_s = H \cdot (T_s(\vec{r}, t) - T_a)$$

✓ Parameters

ρ	: density of tissue [kg·m ³]	SAR	: SAR per unit volume [J/s·kg]
C	: specific heat [J/kg °C]	B	: blood flow [J/s·m ³ °C]
K	: heat transfer [J/s·m° C]	T_b	: blood temperature [°C]
A	: metabolic heat [J/s·m ³]	T_s	: skin temperature [°C]
n	: outward unit vector normal to S	T_a	: surface temperature [°C]
s	: skin surface [m ²]	SW	: the sweat coefficient [W/m ²]
H	: heat transfer coefficient [W/m ² °C]		

IMPROVED EQUATIONS FOR TEMPERATURE RISES

◆ Bio-heat Equation

$$C(\vec{r}) \cdot \rho(\vec{r}) \frac{\partial T(\vec{r}, t)}{\partial t} = \nabla \cdot (K(\vec{r}) \nabla T) + A(\vec{r}, t) + \rho(\vec{r}) \cdot SAR(\vec{r}) - B(\vec{r}, t) \cdot (T(\vec{r}, t) - T_b(t))$$

◆ Boundary condition

$$-K(\vec{r}) \frac{\partial T(\vec{r}, t)}{\partial n} s = H \cdot (T_s(\vec{r}, t) - T_a) + SW(\vec{r}, t)$$

✓ Parameters

ρ	: density of tissue [kg·m ³]	SAR	: SAR per unit volume [J/s·kg]
C	: specific heat [J/kg °C]	B	: blood flow [J/s·m ³ °C]
K	: heat transfer [J/s·m° C]	T_b	: blood temperature [°C]
A	: metabolic heat [J/s·m ³]	T_s	: skin temperature [°C]
n	: outward unit vector normal to S	T_a	: surface temperature [°C]
s	: skin surface [m ²]	SW	: the sweat coefficient [W/m ²]
H	: heat transfer coefficient [W/m ² °C]		

MODELING FOR BLOOD TEMPERATURE

Bio-heat Equation

$$C(\vec{r}) \cdot \rho(\vec{r}) \frac{\partial T(\vec{r}, t)}{\partial t} = \nabla \cdot (K(\vec{r}) \nabla T) + A(\vec{r}, t) + \rho(\vec{r}) \cdot SAR(\vec{r}) - B(\vec{r}, t) \cdot (T(\vec{r}, t) - T_b(t))$$

Conventional bio-heat equation

T_b : constant

→ Thermodynamic law is not satisfied.

In this study

T_b (blood temperature [°C])

T_b is changed according to the equation in order to satisfy the thermodynamic law

$$T_b(t) = T_b(0) + \int_0^t \frac{1}{V_b \cdot C_b \cdot \rho_b} \left\{ \int_V (A(\vec{r}, t) + \rho(\vec{r}) \cdot SAR(\vec{r})) dV - \int_s (H(T_s(\vec{r}, t) - T_a) + SW(\vec{r}, t)) \cdot ndS \right\} dt - \frac{1}{V_b \cdot C_b \cdot \rho_b} \int_V C(\vec{r}) \cdot \rho(\vec{r}) \cdot (T(\vec{r}, t) - T(\vec{r}, 0)) dV$$

$\rho_b(3900)$: density of blood [kg/m³] $C_b(1058)$: specific heat of blood [J/kg °C]
 $V_b(0.005)$: volume of blood [m³]

THERMOREGULATION MODELING: BLOOD FLOW

Bio-heat Equation

$$C(\vec{r}) \cdot \rho(\vec{r}) \frac{\partial T(\vec{r}, t)}{\partial t} = \nabla \cdot (K(\vec{r}) \nabla T) + A(\vec{r}, T(\vec{r}, t)) + \rho(\vec{r}) \cdot SAR(\vec{r}) - B(\vec{r}, t) \cdot (T(\vec{r}, t) - T_b(\vec{r}, t))$$

In this study

All tissues except the skin

$$B(\vec{r}, T(\vec{r}, t)) = \cdot B_0(\vec{r}) \quad @ T(\vec{r}) \leq 39$$

$S_b(0.8)$: coefficient B_0 : basal blood flow

M.Hoque et al, IEEE Trans. Biomed.Eng., (1988.6).

The skin

$$B(\vec{r}, T(\vec{r})) = \left[B_0(\vec{r}) + F_{HB} (T_H - T_{H0}) + F_{SB} \overline{\Delta T_s} \right] \times 2^{(T(\vec{r}) - T_0(\vec{r})) / 6}$$

$F_{HB}(17500)$: coefficient [W/°C · m³]

T_0 : basal skin temperature per unit volume

$F_{SB}(1100)$: coefficient [W/°C · m³]

T : skin temperature per unit volume [°C]

T_{H0} : temperature in Hypothalamus [°C] ΔT_s : average skin temperature increase [°C]

T_{HO} : basal temperature in Hypothalamus [°C]

R. J. Spiegel, IEEE Trans. Microwave Theory Tech., (1984.8).

UNCERTAINTY IN HF DOSIMETRY

Uncertainty, defined by ISO/IEC Guide 98, is usually evaluated with its expanded value which covers **95% confidential interval** of the probability distribution of the evaluated result. Uncertainty of EMF dosimetry depends on many factors. **30% or 1 dB** may be a reasonable target for a specific case with a technique of state of the art in HF region while larger uncertainty has been recognized in LF region, i.e., 3-dB reduction factor due to the uncertainty of the dosimetry is considered in deriving RLs in LF region.

Uncertainty of HF numerical dosimetry and other factors considered in the reduction factor

Uncertainty of numerical techniques;

- Approximation of Maxwell's eq.,
- Boundary conditions,
- Convergence,
- Post processing (local averaging).

Uncertainty of discrete modeling;

- Approximation with staircase of smooth shape,
- Spatial resolution vs complex heterogeneous structure.

Variation of a human body, population;

- Size and weight,
- Internal structure (fat thickness).

Variation of exposure conditions;

- Polarization and direction,
- Reflection and grounding,
- Other source conditions.

Other factors to be considered.

Reduction factor

UNCERTAINTY IN LF REGION

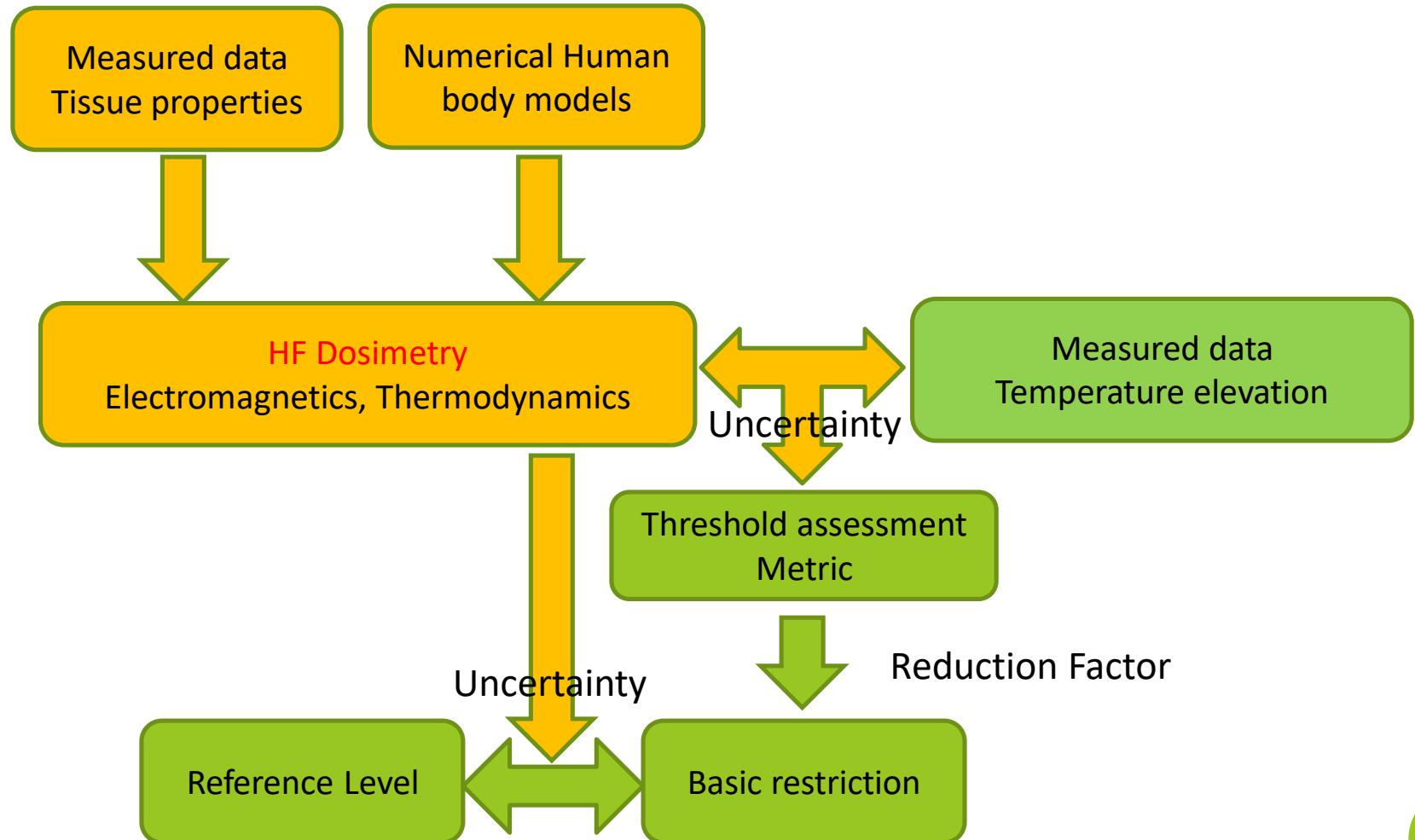
Sec. REFERENCE LEVELS

“An additional reduction factor of 3 was applied to these calculated values to allow for dosimetric uncertainty.”

If we can reduce this uncertainty, an allowable external field level can be relaxed by a factor of 3.

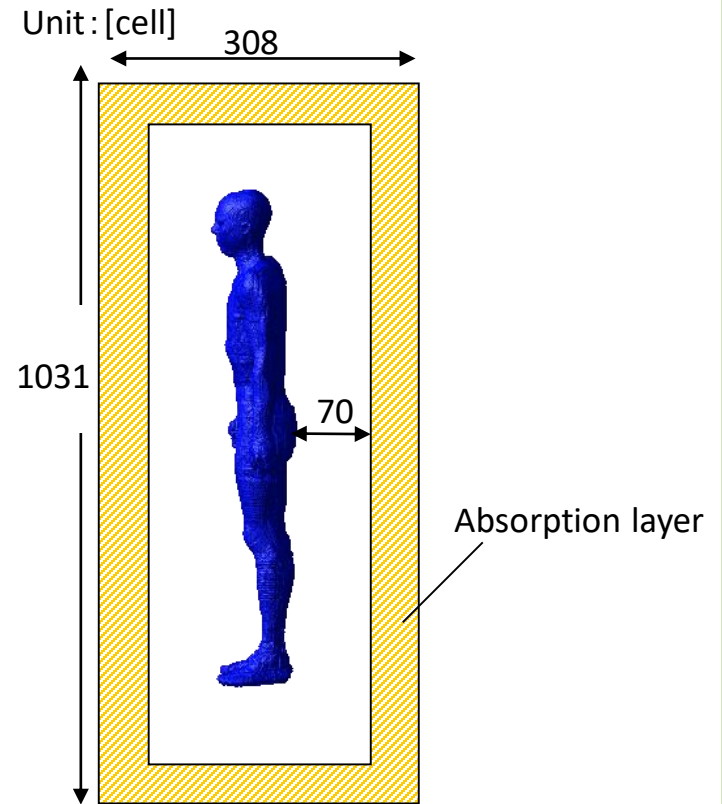
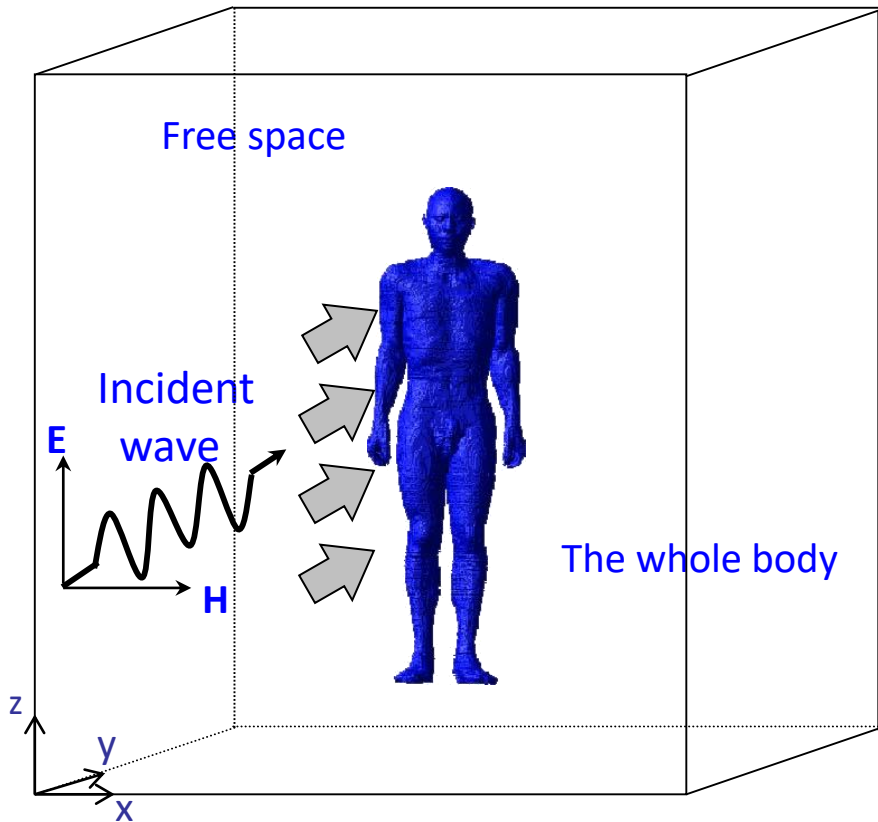
ICNIRP STATEMENT—GUIDELINES FOR LIMITING EXPOSURE TO TIME-VARYING ELECTRIC AND MAGNETIC FIELDS (1 HZ TO 100 KHZ), Health Phys. 2010.

SUMMARY OF COMPUTATIONAL UNCERTAINTY



3. Computational Examples for Human Safety Assessment

WHOLE-BODY EXPOSURE SCENARIOS

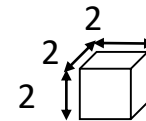


Absorbing boundary condition: UPML

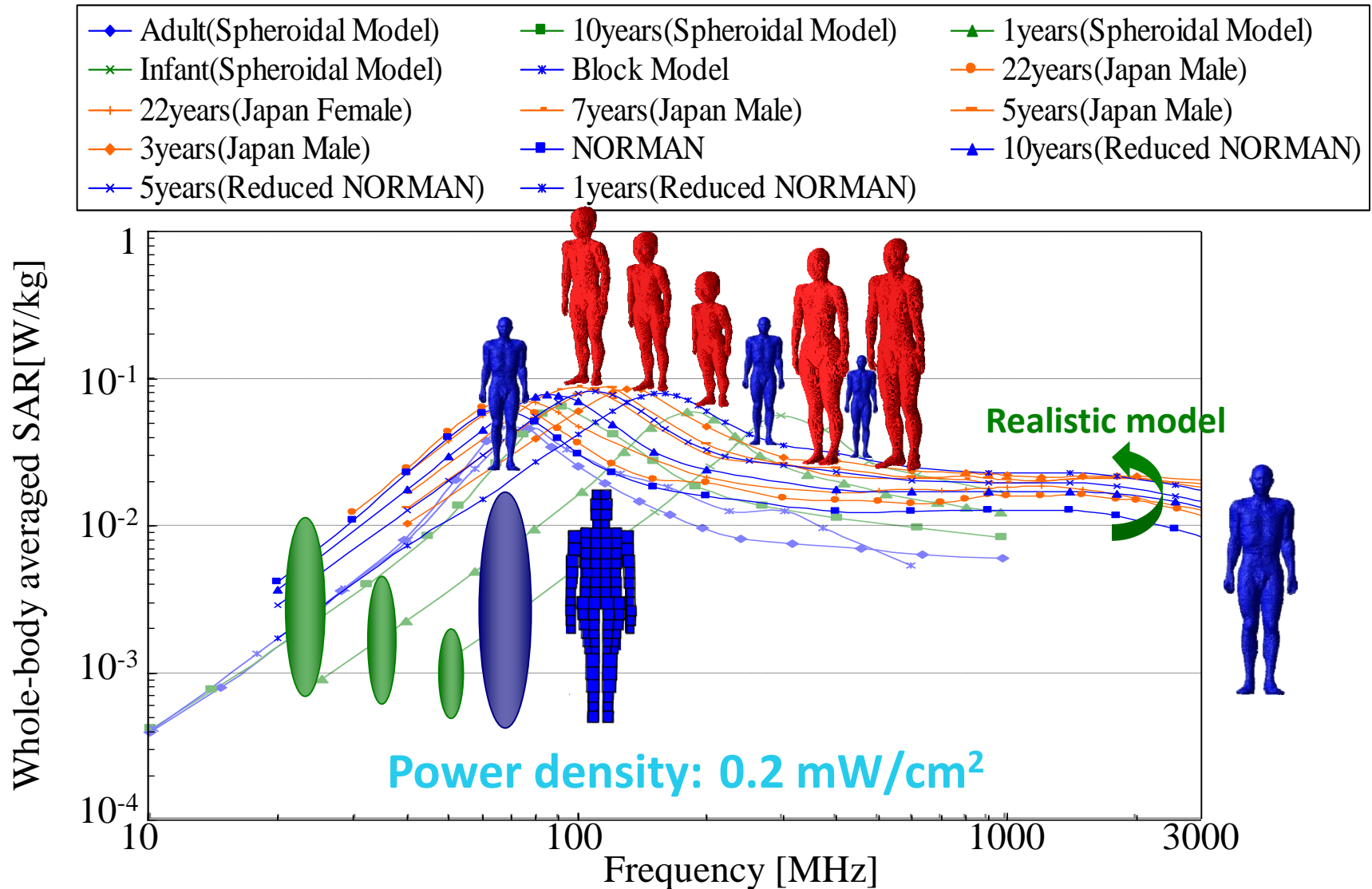
Polarization : Vertical

Cell size

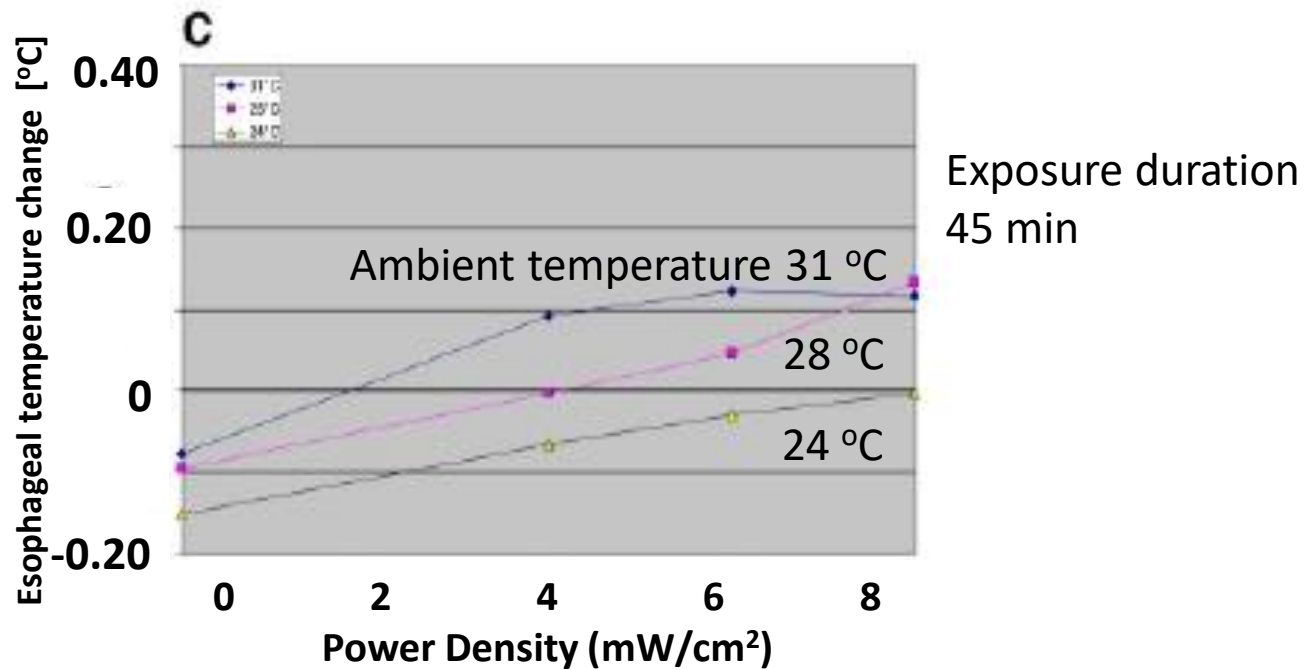
Unit: [mm]



WBA-SAR IN ADULT AND CHILD MODELS



THERMAL DOSIMETRY FOR **WHOLE-BODY** EXPOSURE: BACK EXPOSED AT 100 MHz



Whole-body average (WBA) SAR at 0.68 W/kg for duration of 45 min.

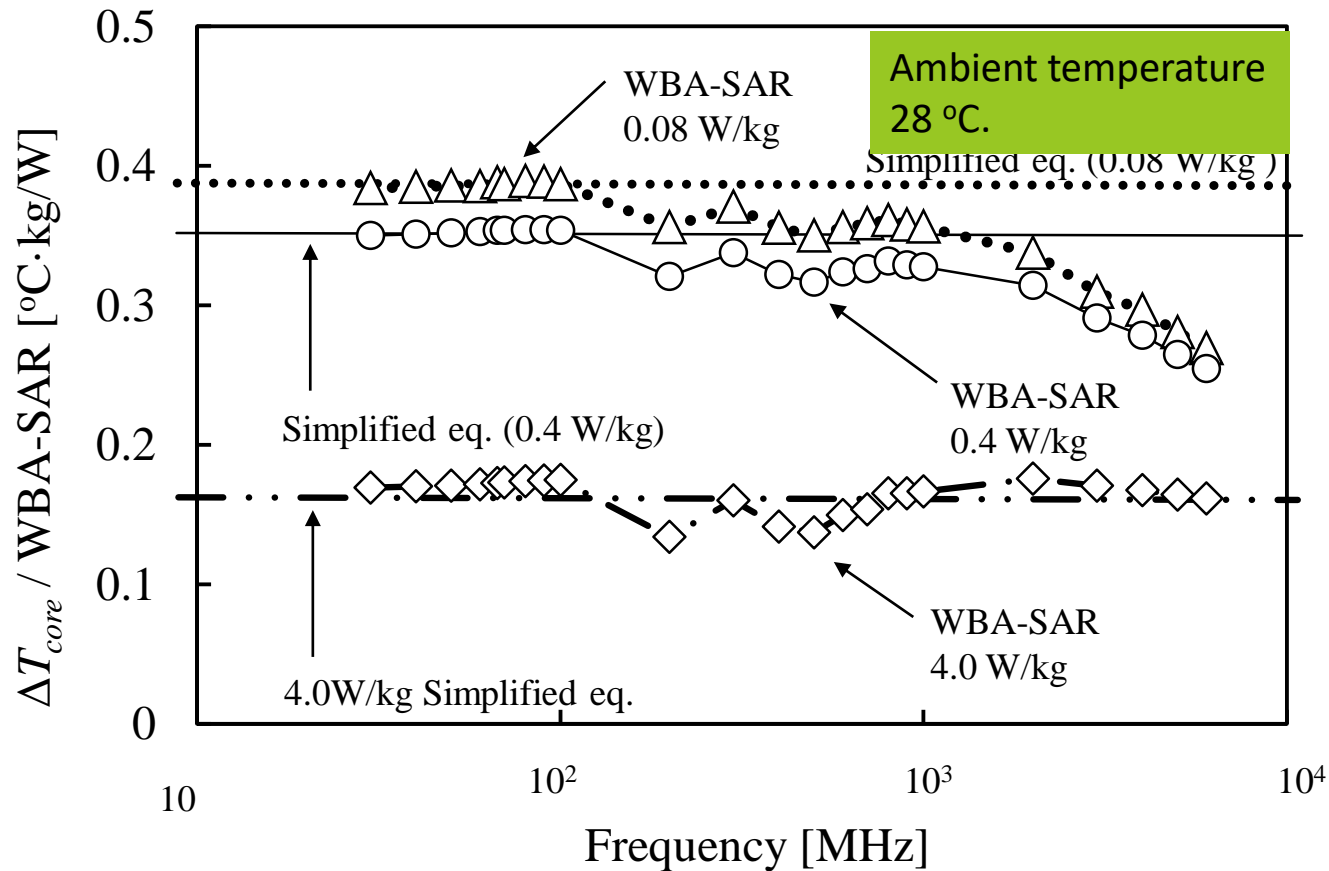
Measured $\Delta T = 0.15\text{-}0.20\text{ }^{\circ}\text{C}$ (100 MHz) Adair

Computed $\Delta T = 0.177\text{ }^{\circ}\text{C}@28\text{ }^{\circ}\text{C}$ (65 MHz) unpublished

Computed $\Delta T = 0.17\text{ }^{\circ}\text{C}@28\text{ }^{\circ}\text{C}$ (100 MHz) by Nelson

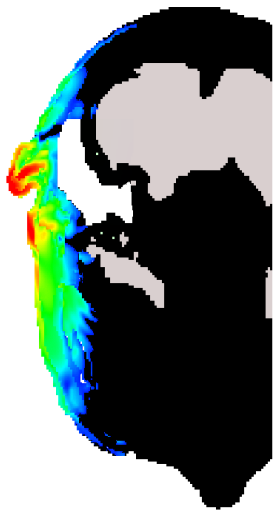
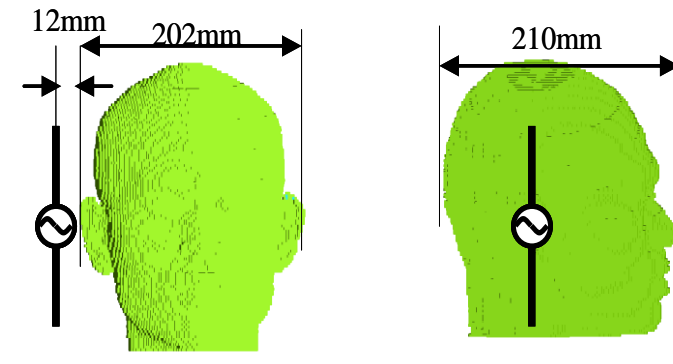
Adair et al, Bioelectromagnetics, 2003
Hirata et al, Phys. Med. Biol., 2007.
Laakso & Hirata, Phys. Med. Biol., 2011.
Nelson et al, Phys. Med. Biol., 2014

CORE TEMPERATURE ELEVATION NORMALIZED BY WBA-SAR

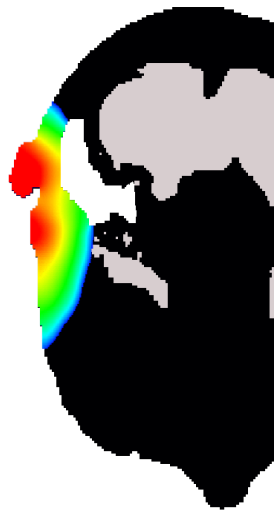


In the elderly, thermoregulatory response is weaker than that in the young adult due to declined heat sensitivity etc, resulting in higher core temperature.

LOCAL TEMPERATURE ELEVATION IN ANATOMICAL HEAD MODELS



SAR

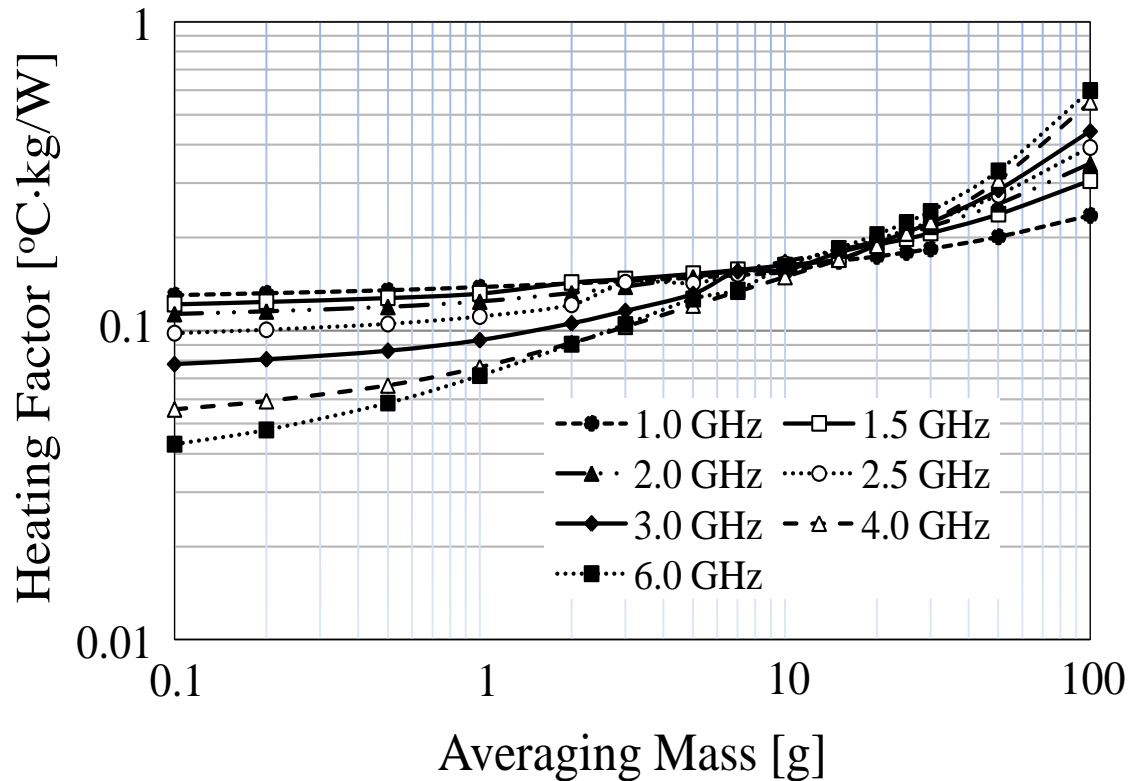


ΔT

- Frequency=6 GHz
- Thermal steady state (~30 min); depending on the frequency
- Temperature elevation distribution in the human model is smoother than that of SAR due to heat diffusion.

- ◆ Wang and Fujiwara (IEEE MTT,1999)
- ◆ Leeuwen et al.(Phys.Med.Biol.1999)
- ◆ Bernardi et al. (IEEE MTT, 2000)
- ◆ Wainwright(Phys.Bio.Med.2000)
- ◆ Gandhi et al. (IEEE MTT, 2001)
- ◆ Hirata et al. (IEEE EMC, 2003)
- ◆ Samaras et al. (IEEE EMC, 2007)
- ◆ McIntosh et al. (BEMS, 2010)

EFFECT OF AVERAGING MASS: AVERAGED SAR VS TEMPERATURE ELEVATION



The heating factors converge at the averaging mass of ~ 10 g.
 ΔT can be estimated in terms of SAR at different frequencies.

Hirata et al, Phys. Med. Biol., 2009

The blood flow may increase for the temperature elevation caused by local exposure.
The heating factors without considering the response are conservative.

Alekseev et al, BEMS, 2005

TEMPERATURE ELEVATION FOR MILLIMETER WAVE EXPOSURE

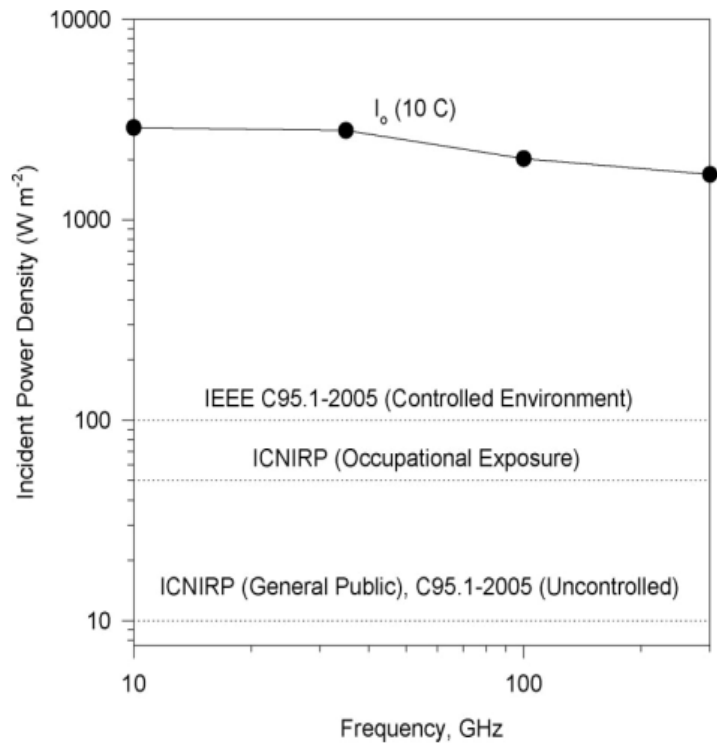


Fig. 1. Incident power density sufficient to increase skin temperature by 10°C, considered to be the threshold for thermal pain. Also shown are IEEE C95.1-2005 and ICNIRP exposure limits.

Foster et al, Health Phys., 2010

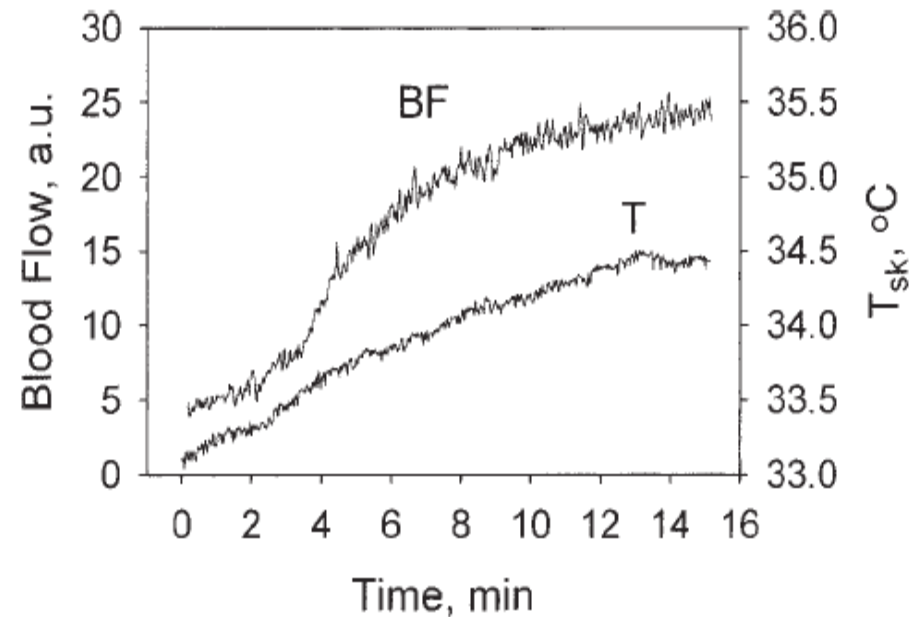
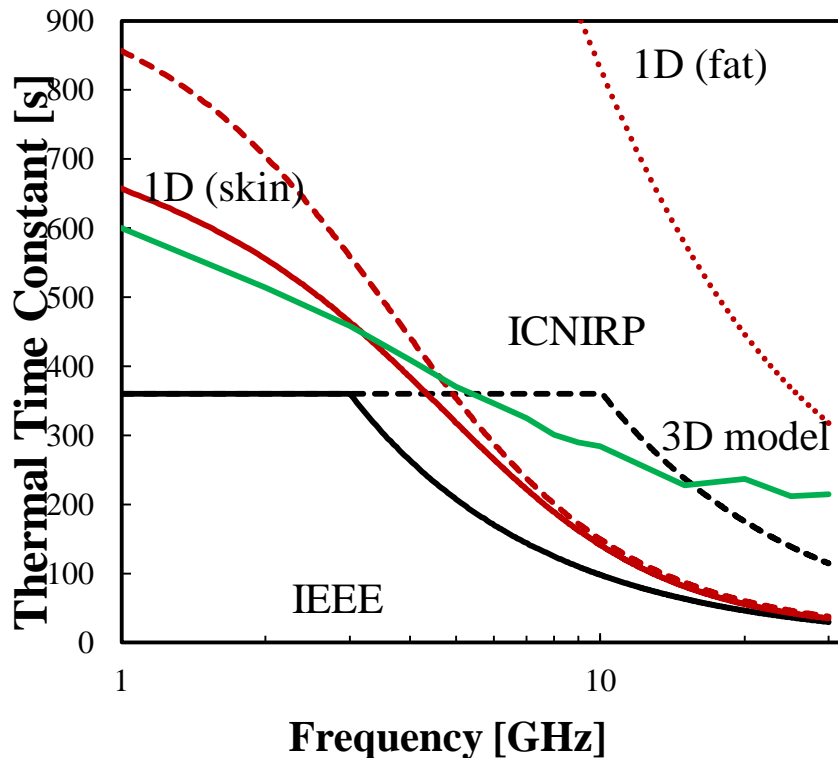


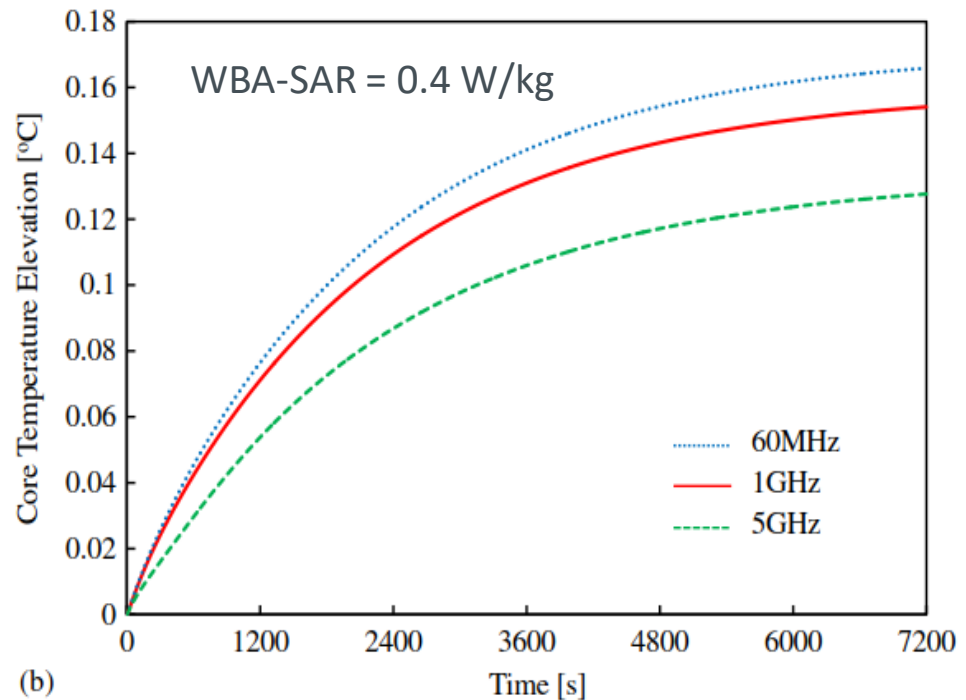
Fig. 7. Blood flow (BF) and temperature (T) changes in the forearm skin following a vasodilator cream (nicoboxil/nonivamid) application.

Alekseev et al, Bioelectromagnet., 2005

THERMAL TIME CONSTANTS FOR LOCAL AND WHOLE-BODY EXPOSURES



Foster et al, Bioelectromagnetics, 1998

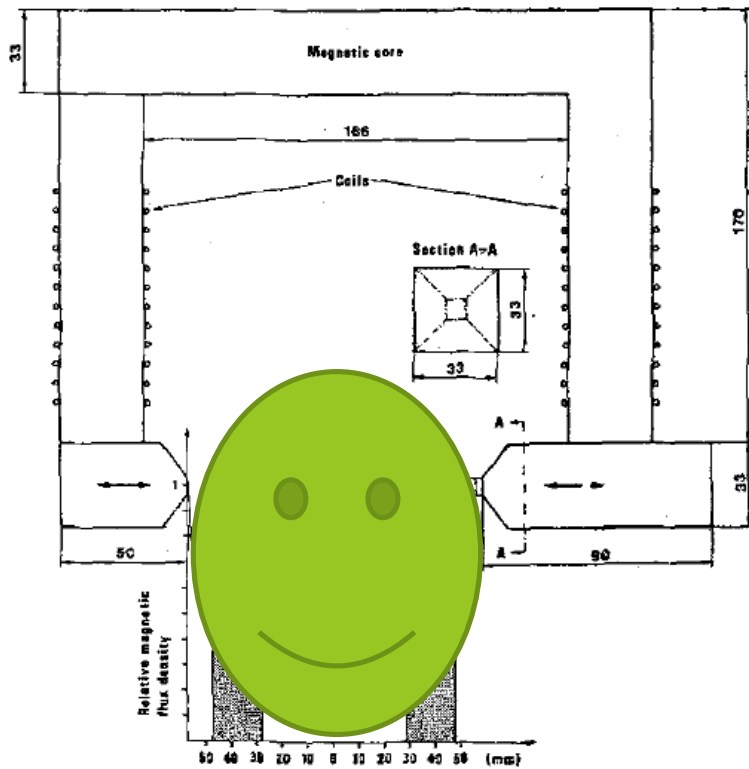


Hirata et al, Phys. Med. Biol., 2013

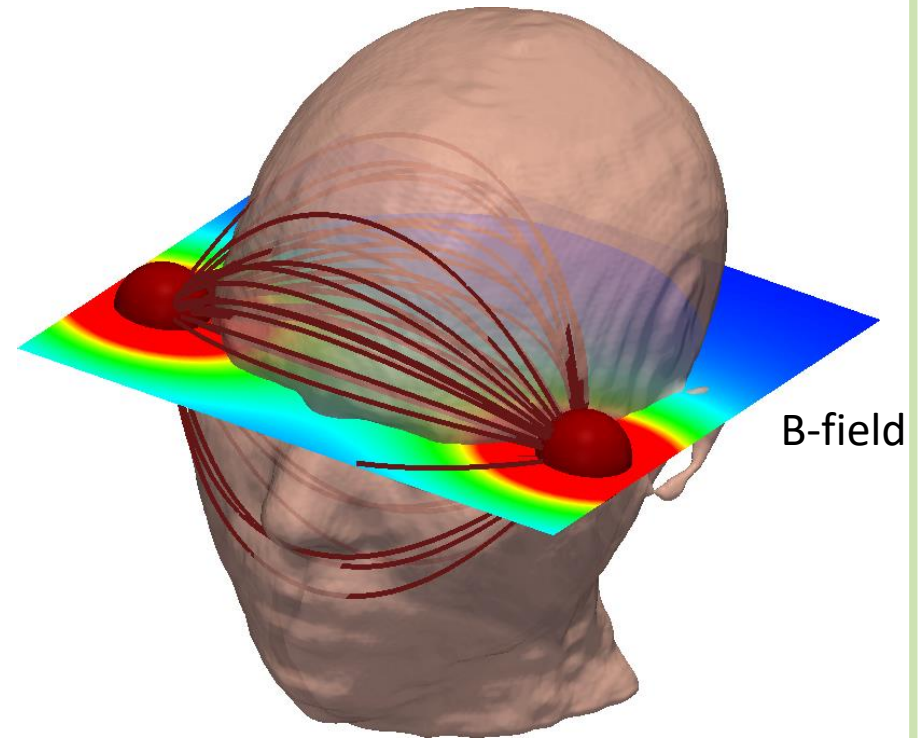
MAGNETOPHOSPHENES (CNS STIMULATION) (EM MODELING)

Laakso and Hirata, Phys. Med. Biol., 2012

Experimental setup



Computation setup

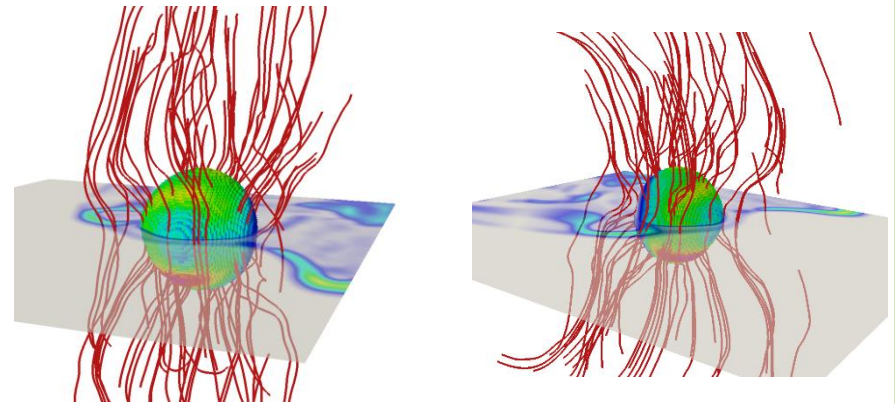
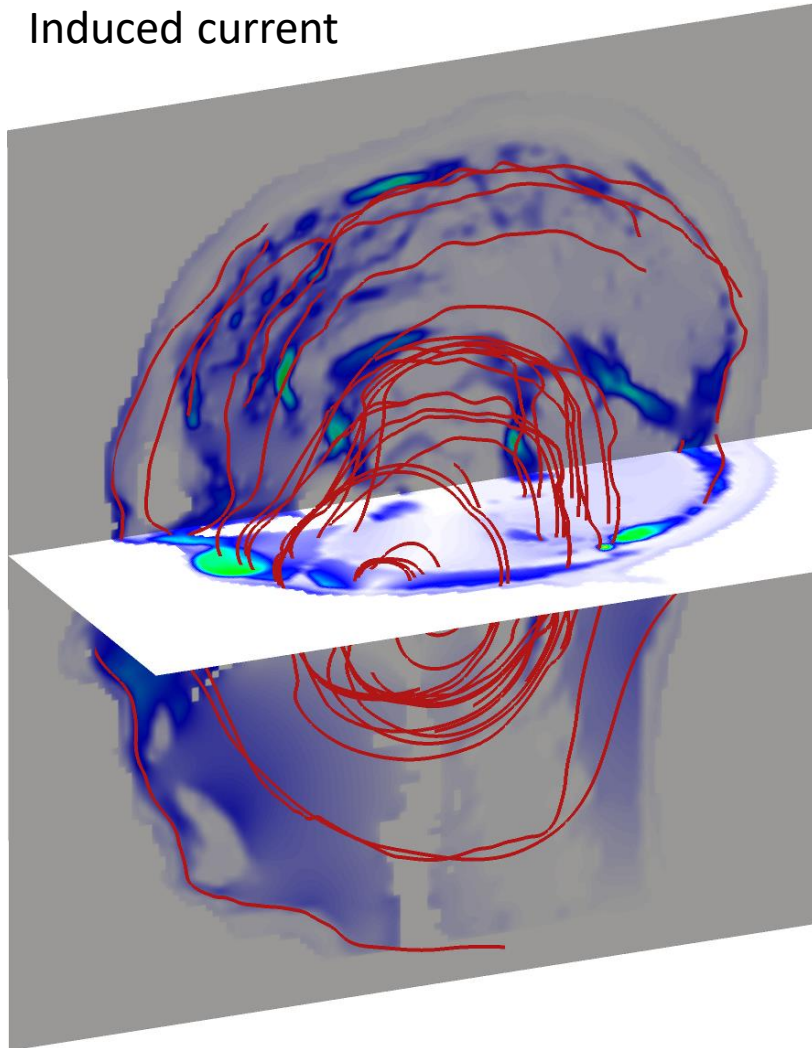


Five anatomical models
0.5 mm resolution

Lövsund P, Öberg P, Nilsson S and Reuter T 1980
Magnetophosphenes: a quantitative analysis of thresholds
Med. Biol. Eng. Comput. **18** 326-34

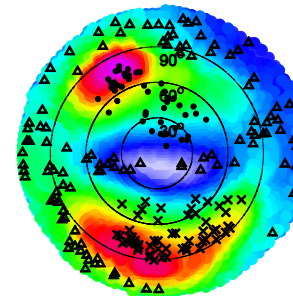
COMPUTATIONAL RESULTS FOR MAGNETOPHOSPHEN

Induced current

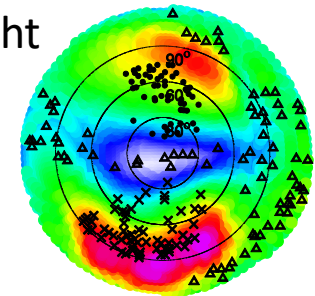


Induced current on the retinas

left



right



up

down

The lowest threshold current density for magnetophosphenes is $\sim 10 \text{ mA/m}^2$ (radial to the eyeball)

current concentrates at the eyes
(high conductivity)

- *How reliable are the computational results?*
 - For five anatomically based models, variability of induced current density was $\pm 30\%$ or less.
- *What is the primary difference between ellipsoidal model and anatomically based models?*
 - In ellipsoidal model, the maximum field appears **around the surface**.
 - In anatomically-based model, the maximum current appeared **around the eye** due to its high conductivity. The main component is radial, thus **the induced electric field is derived by dividing the current by the conductivity**.

Example of Product Safety Assessment

- Wireless Power Transfer-

References:

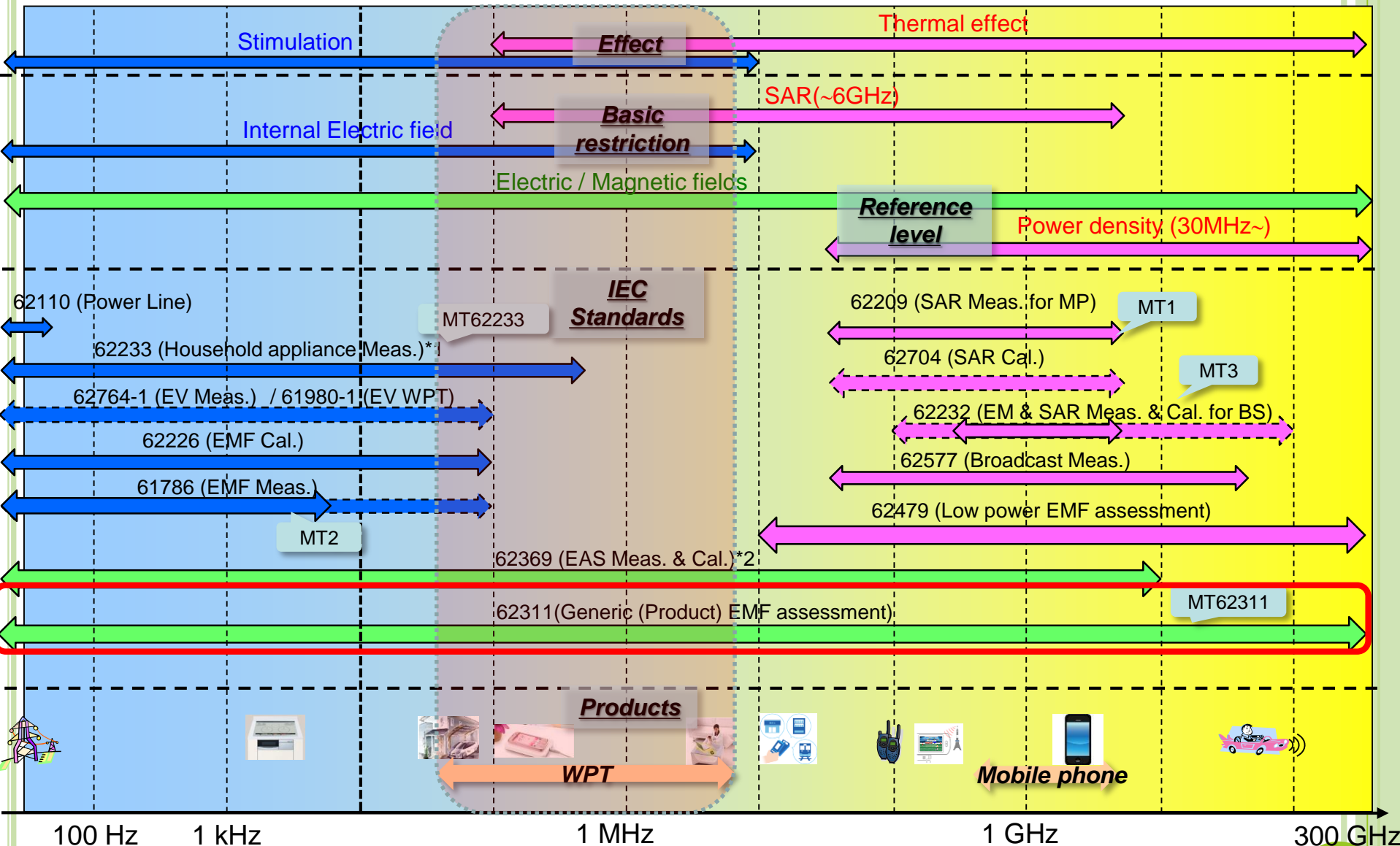
- I. Laakso, S. Tsuchida, A. Hirata, and Y. Kamimura, “Evaluation of SAR in a human body model due to wireless power transmission in the 10 MHz band,” *Physics in Medicine and Biology*, vol.57, pp.4991-5002, Jul. 2012.
- T. Shimamoto, I. Laakso, and A. Hirata, “In-situ electric field in human body model in different postures for wireless power transfer system in an electrical vehicle,” *Physics in Medicine and Biology*, vol.60, no.1, pp.163-174, 2015.
- T. Shimamoto, I. Laakso, and A. Hirata, “Internal electric field in pregnant-woman model for wireless power transfer system in electric vehicle,” *Electronics Letters*, vol.51, no.25, pp.2136-2137, 2015.
- K. Wake, I. Laakso, A. Hirata, J. Chakarothai, S. Watanabe, V. De Santis, M. Feliziani, and M. Taki, “Derivation of coupling factors for different wireless power transfer systems: inter- and intra-laboratory comparison,” *IEEE Transactions on Electromagnetic Compatibility*, vol.59, no.2, pp.677-685, 2017.

EXAMPLE OF WPT SYSTEMS (DISCUSSED IN JAPAN)

	Mobile devices etc.	Mobile devices etc.	EV
Type	Magnetic coupling (resonant)	Capacitive coupling	Magnetic coupling (inductive/resonant)
Frequency	6.765 ~ 6.795 MHz	425 ~ 524 kHz	79 ~ 90 kHz
Power	~ 100 W	~ 100 W	~ 7.7 kW
Distance (Tx-Rx)	~ 30 cm	~ 1 cm	~ 30 cm
Reported on	January 21 st , 2015		July 17 th , 2015



STANDARDS FOR EXPOSURE ASSESSMENT BY IEC TC106



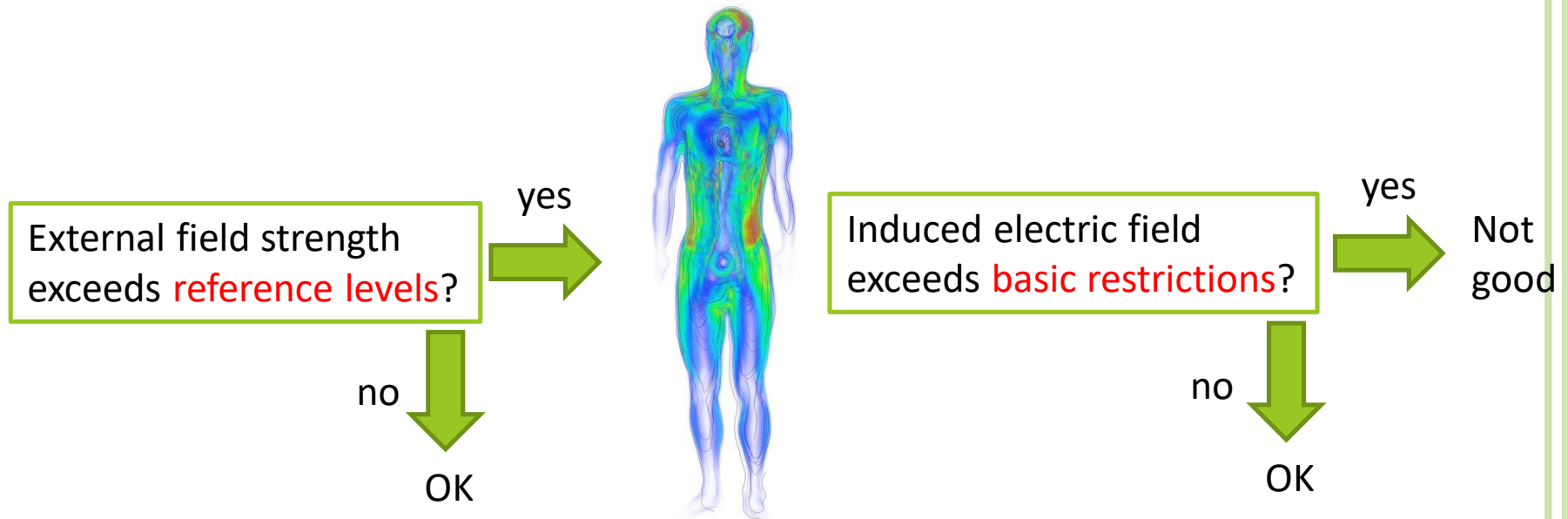
*1; Frequency range up to 300 GHz and electric and magnetic fields are considered. But only magnetic field measurement procedure 10 Hz to 400 kHz is described.

*2; Frequency range up to 300 GHz are considered. But only procedures up to 10 GHz are described.

CONCEPT FOR COMPLIANCE WITH INTERNATIONAL EXPOSURE GUIDELINES/ STANDARDS

e.g.) Limits for human exposure below 100 kHz:

- Reference level: **external field strength**
- Basic restriction: **electric field induced in the body**



† ICNIRP : “Guidelines for limiting exposure to time-varying electric and magnetic field (1Hz to 100kHz)”, Health Phys., vol.99, pp.818-836, 2010.

†† IEEE C95-1 : “IEEE Standard for Safety Levels with Respect to Human Exposure to Radio Frequency Electromagnetic Field, 3kHz to 300GHz” , 2005.

ON WPT COMPLIANCE PROCEDURE

- No specific standards at the moment
- IEC TC106 WG9 (Chaired by Dr. T. Onishi)
- IEC62311:2007

Assessment of electronic and electrical equipment related to human exposure restrictions for electromagnetic fields (0 Hz - 300 GHz)

Target Frequencies

- Electric vehicles (85 kHz)
- Laptop computer etc
6.78 MHz
- LF or HF ?

LF



H-field measurement

HF



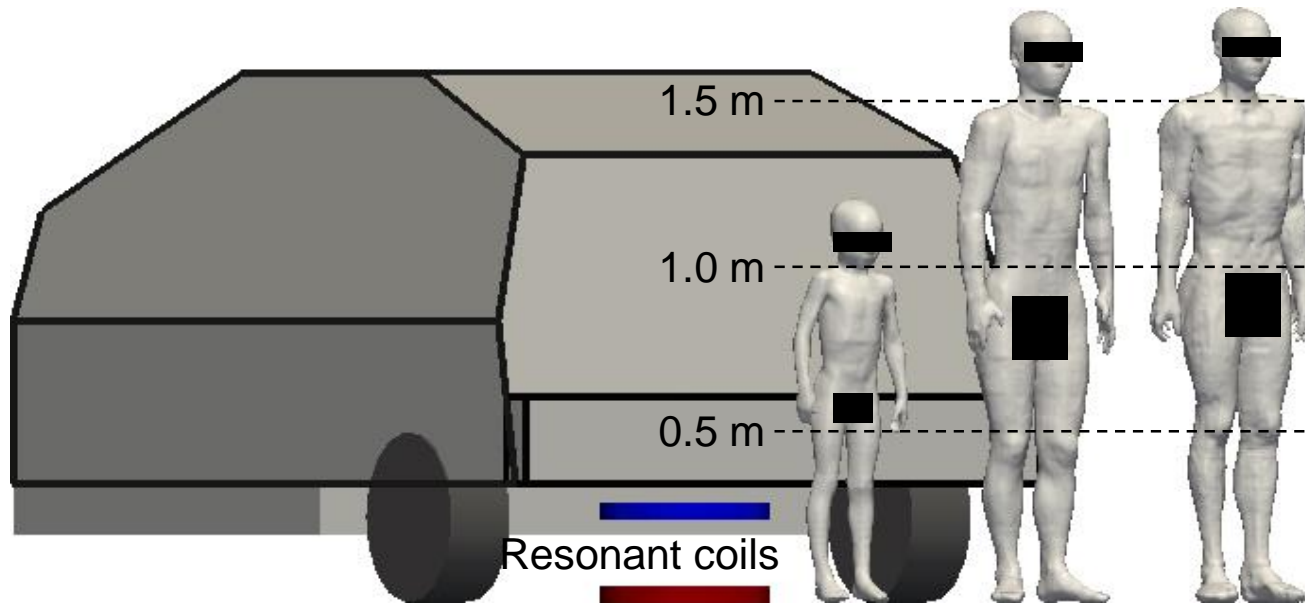
SAR measurement

EXPOSURE FROM WPT IN ELECTRIC VEHICLES

- Finite-element method with 2 mm cubical elements

➤ 7.7 kW

➤ 75 kHz



Three numerical **body models**:

Thelonious

TARO

NORMAN

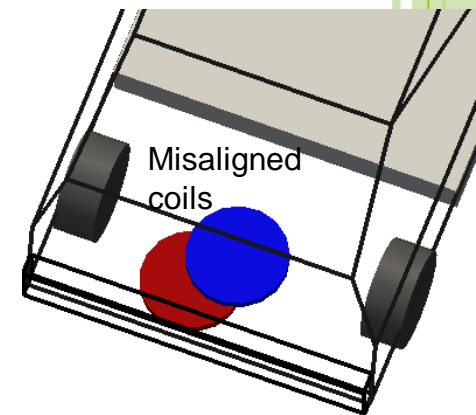
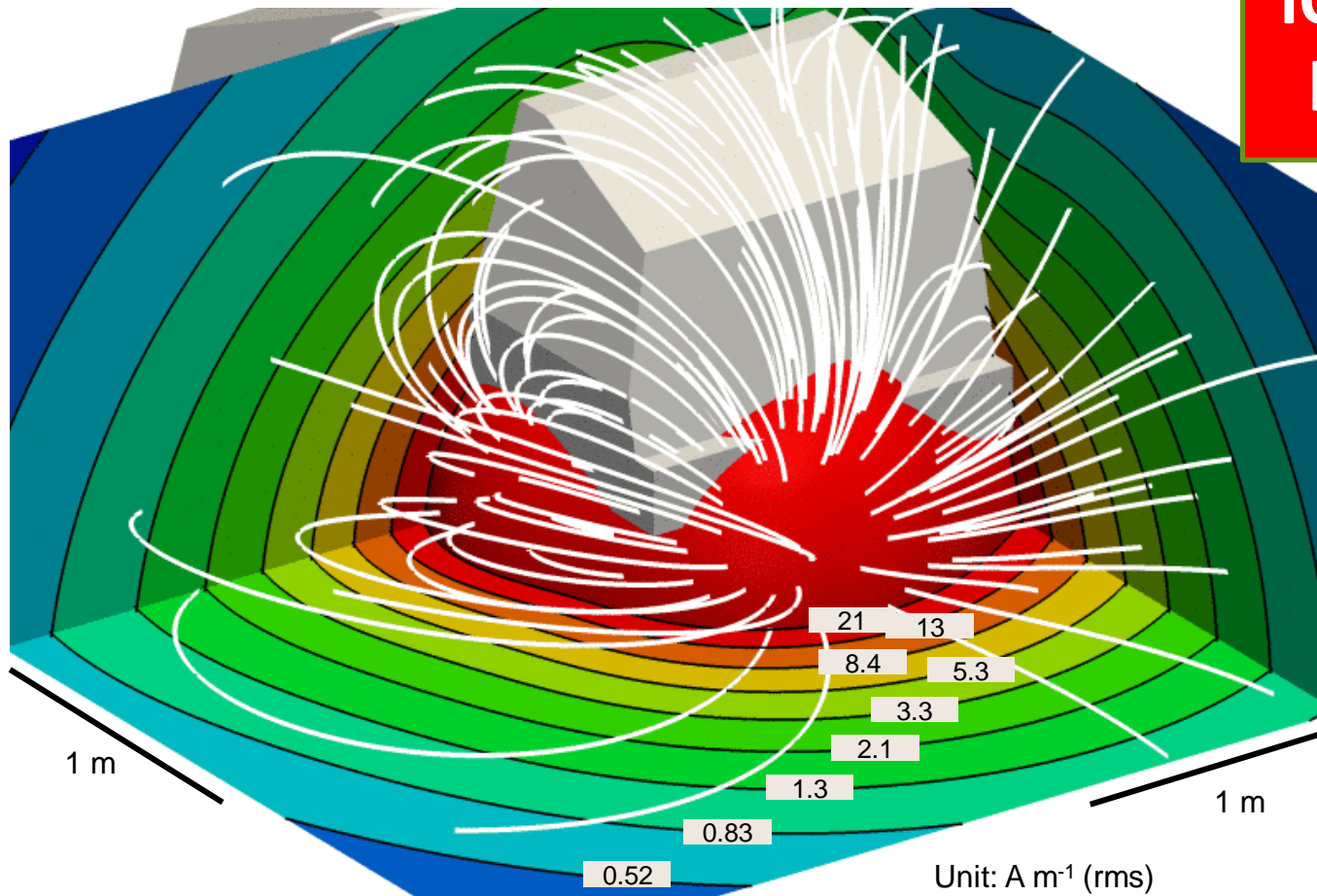
IT'IS,
Switzerland

NICT,
Japan

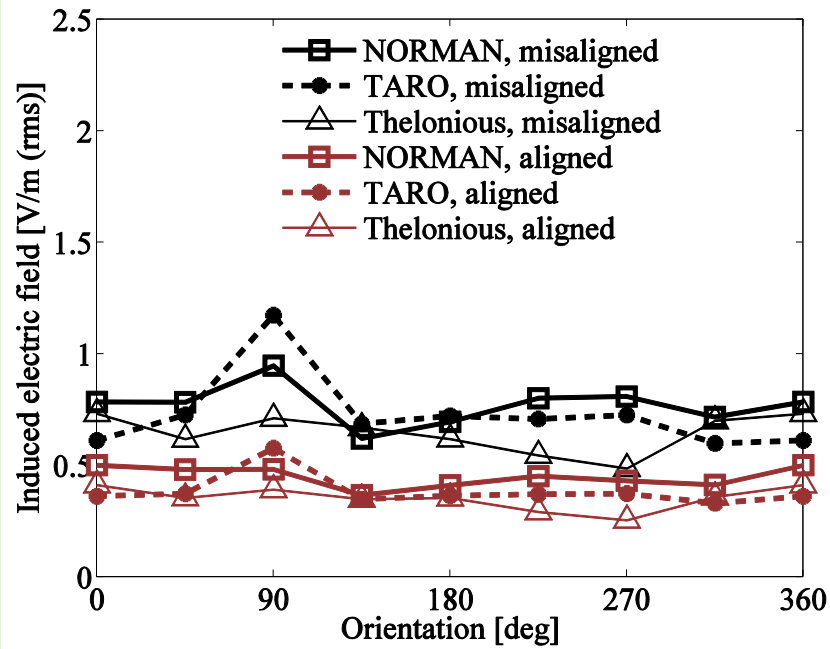
HPA,
UK

COMPUTED MAGNETIC FIELD FROM EV

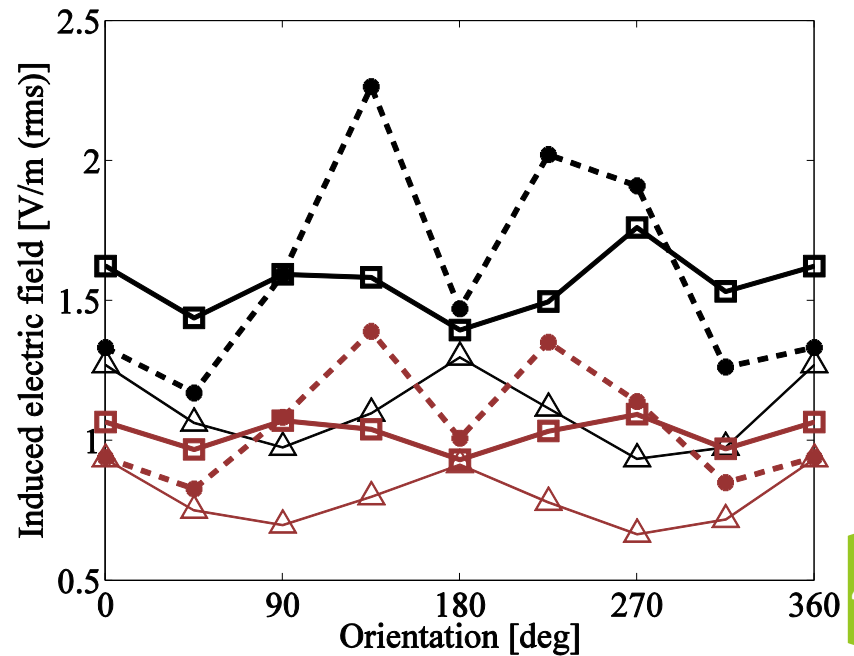
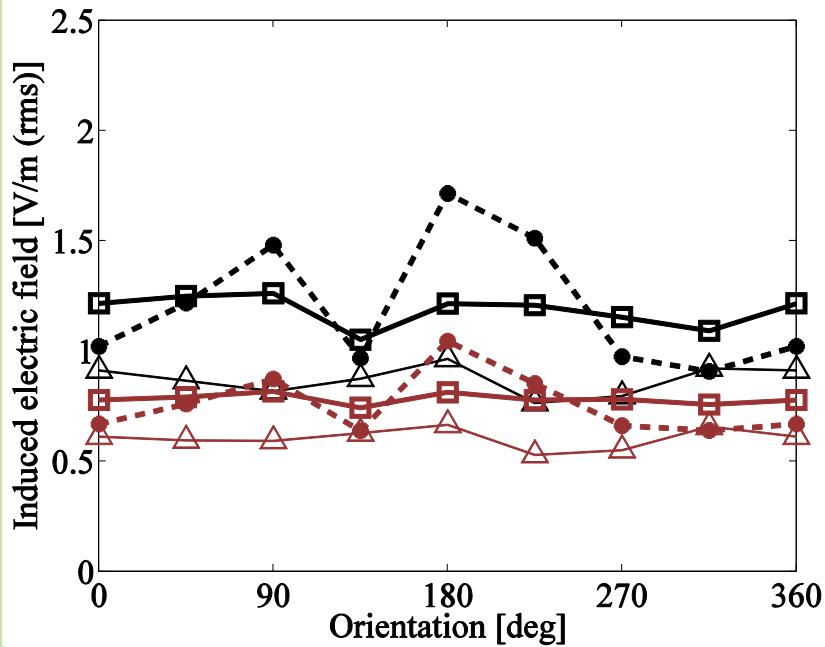
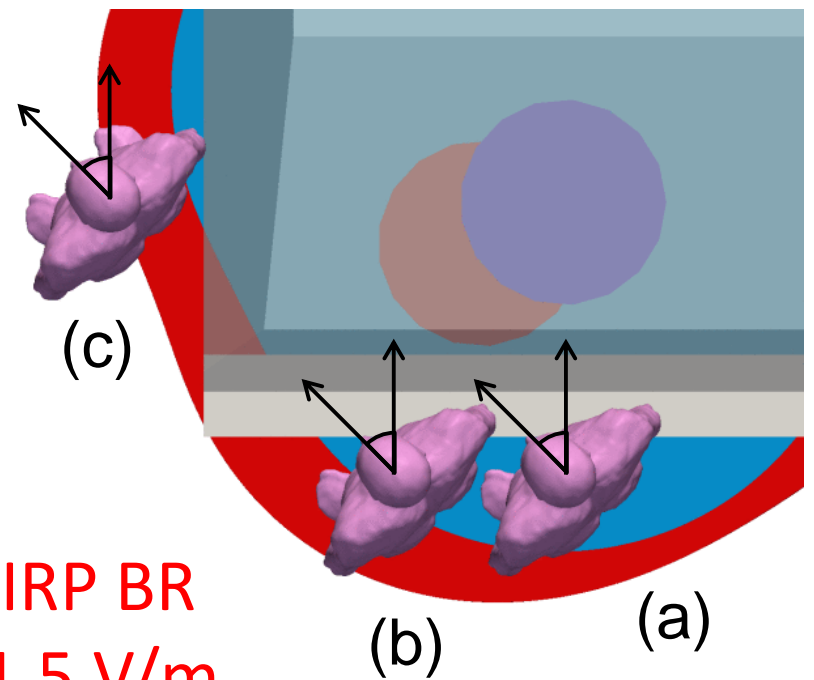
ICNIRP reference level = 21 A/m



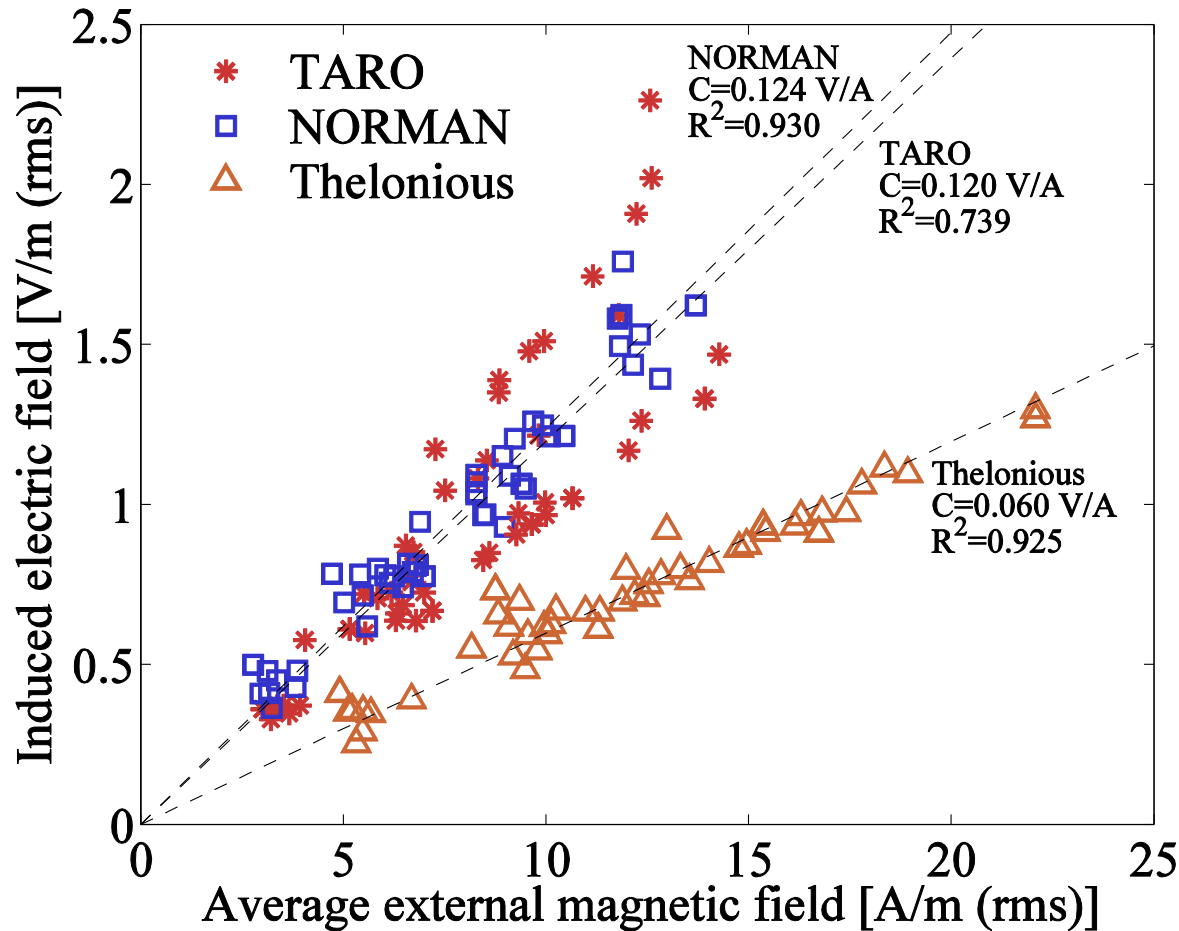
- Solid red represent a region where the reference level of ICNIRP is not satisfied.



ICNIRP BR
= 11.5 V/m

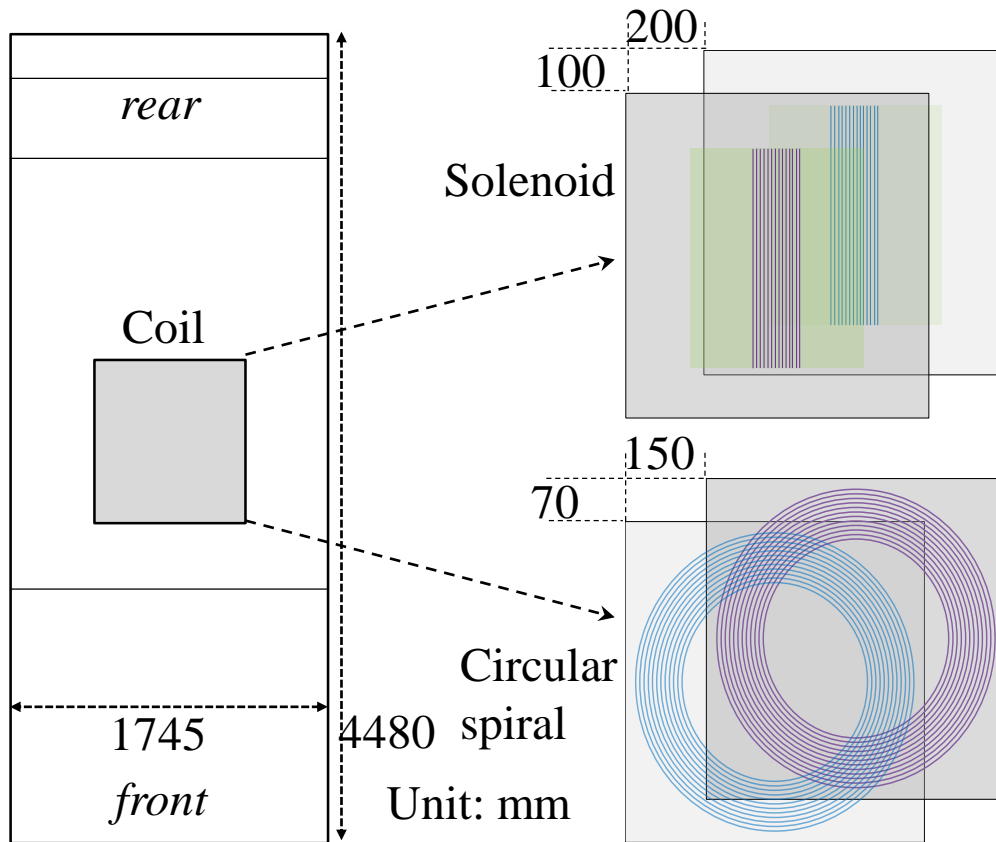


INDUCED ELECTRIC FIELD CORRELATES WITH THE EXTERNAL MAGNETIC FIELD (AVERAGE OVER THE WHOLE BODY)



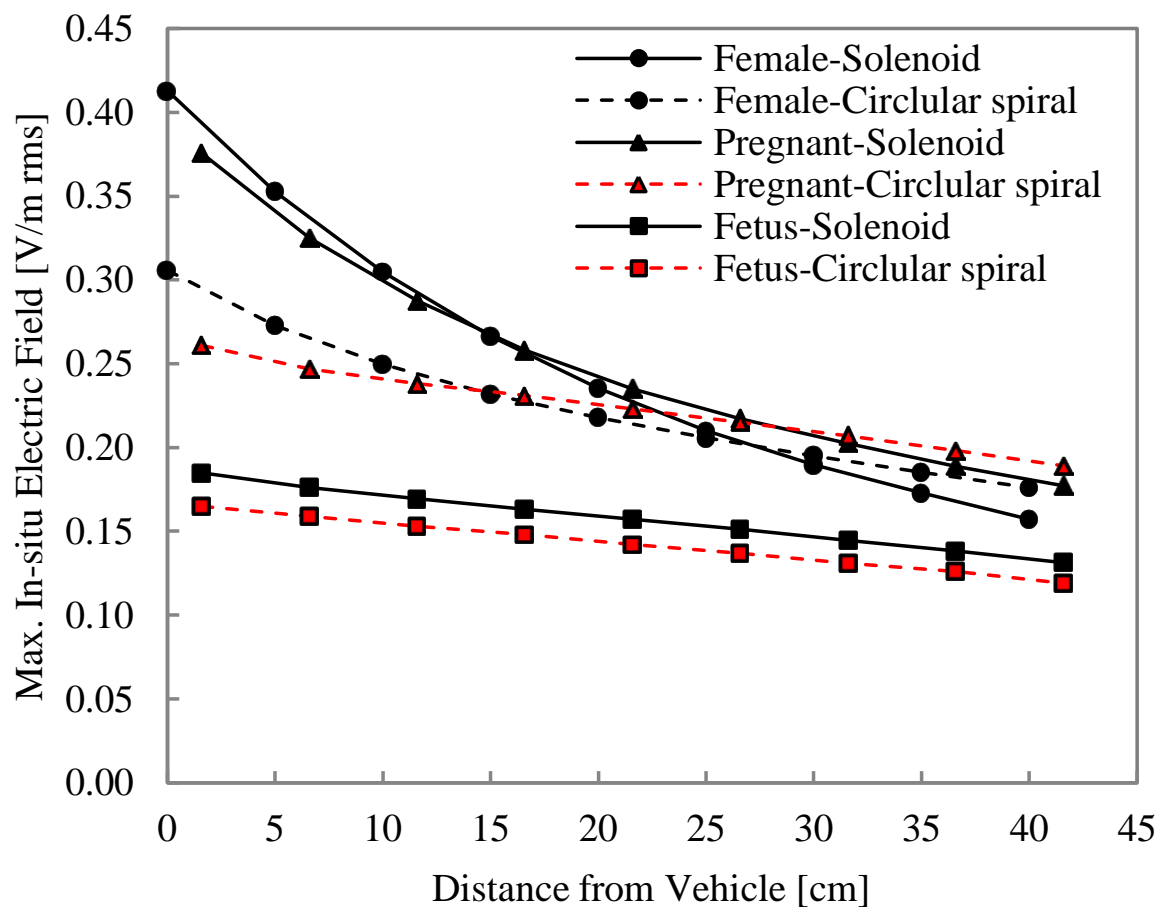
Induced field in child is smaller than that in the adult.
Magnetic flux passing through the body is important.

PARAMETERS OF COUPLING COILS IN EV



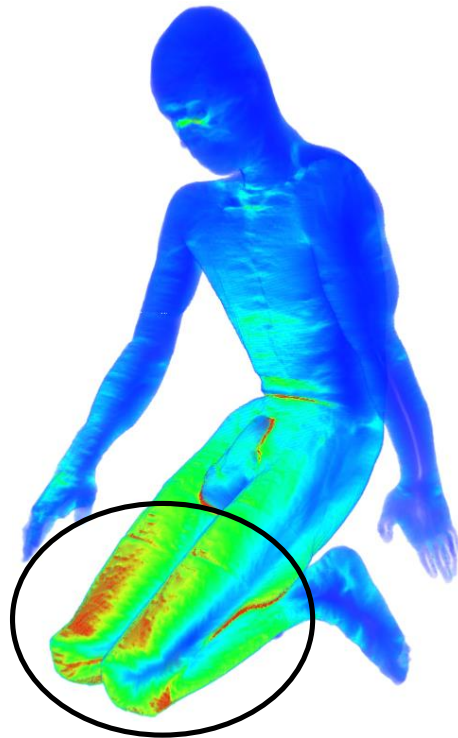
	Solenoid	Circular spiral
Loop number	14	12
Core size	Width: 405mm Height: 325mm	Diameter Outer: 520mm Inner: 350mm
Magnetic material	Relative permeability: 1800 Conductivity: 0.33 S/m	
Distance between coils	120mm	170mm

DISTANCE DEPENDENCY OF IN-SITU ELECTRIC FIELD IN STANDING HUMAN BODY MODELS



EXPOSURE SCENARIO 2:

Peak E: 0.965 V m^{-1}



(i) Solenoid

Peak E: 0.526 V m^{-1}



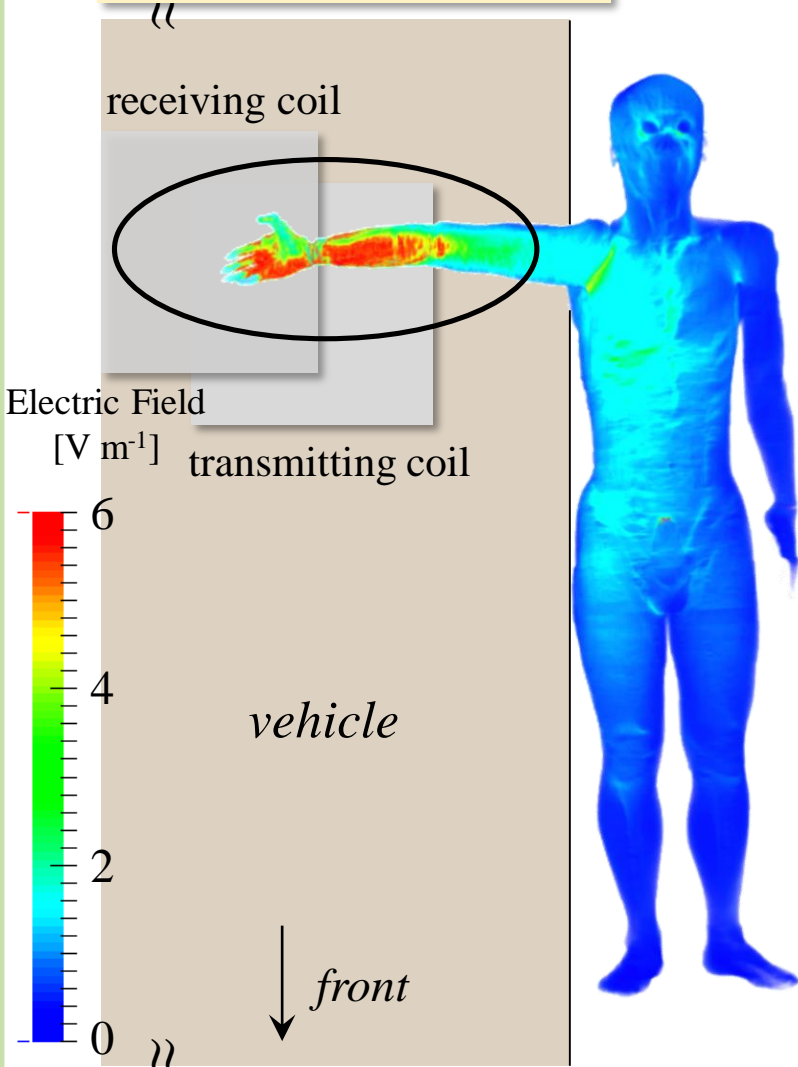
(ii) Circular spiral

Electric Field
[V m^{-1}]

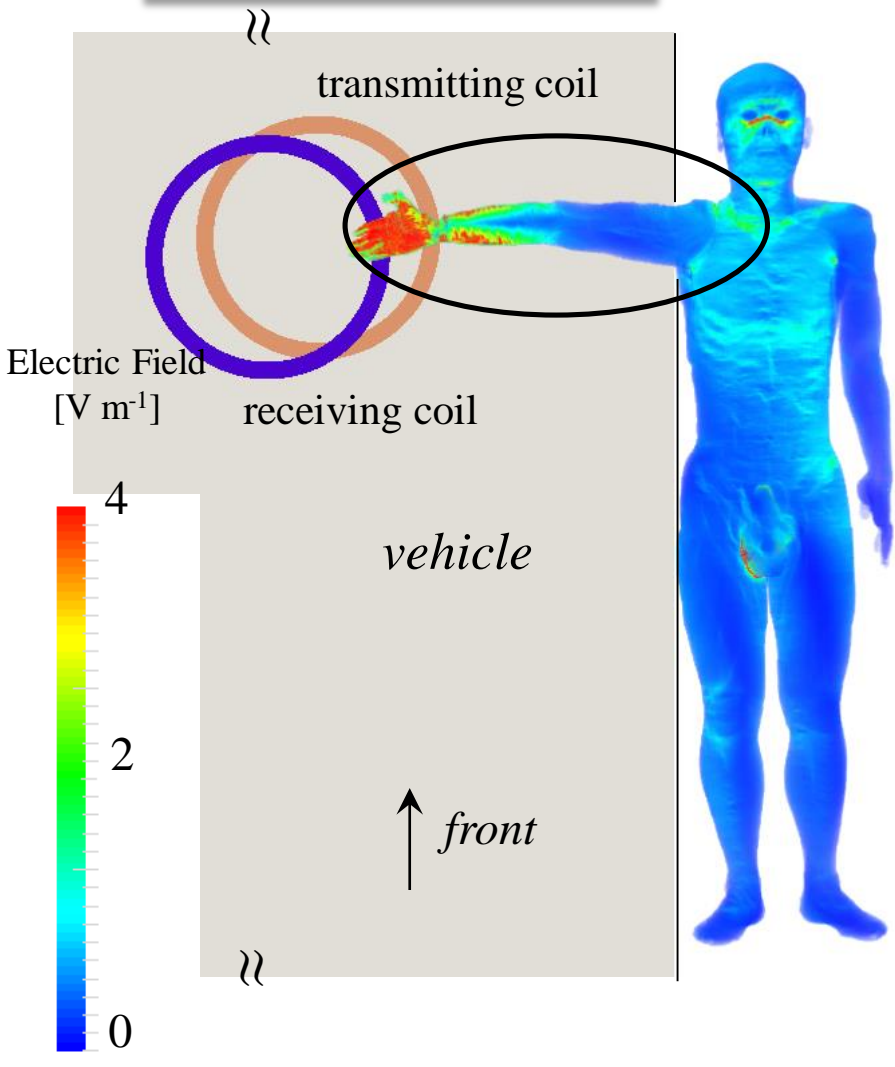


EXPOSURE SCENARIO 3:

➤ Peak E: 6.24 V m^{-1}

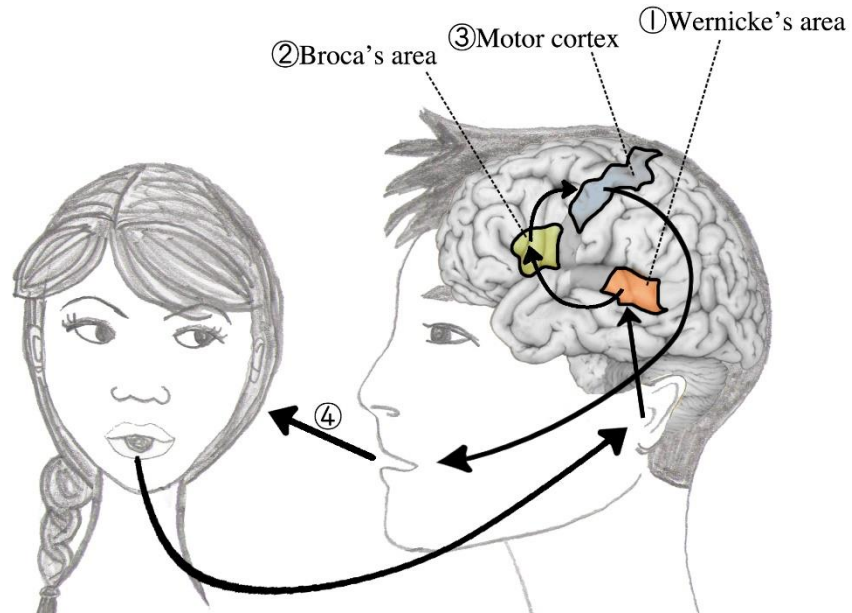


➤ Peak E: 4.20 V m^{-1}

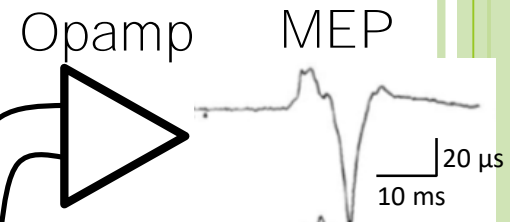
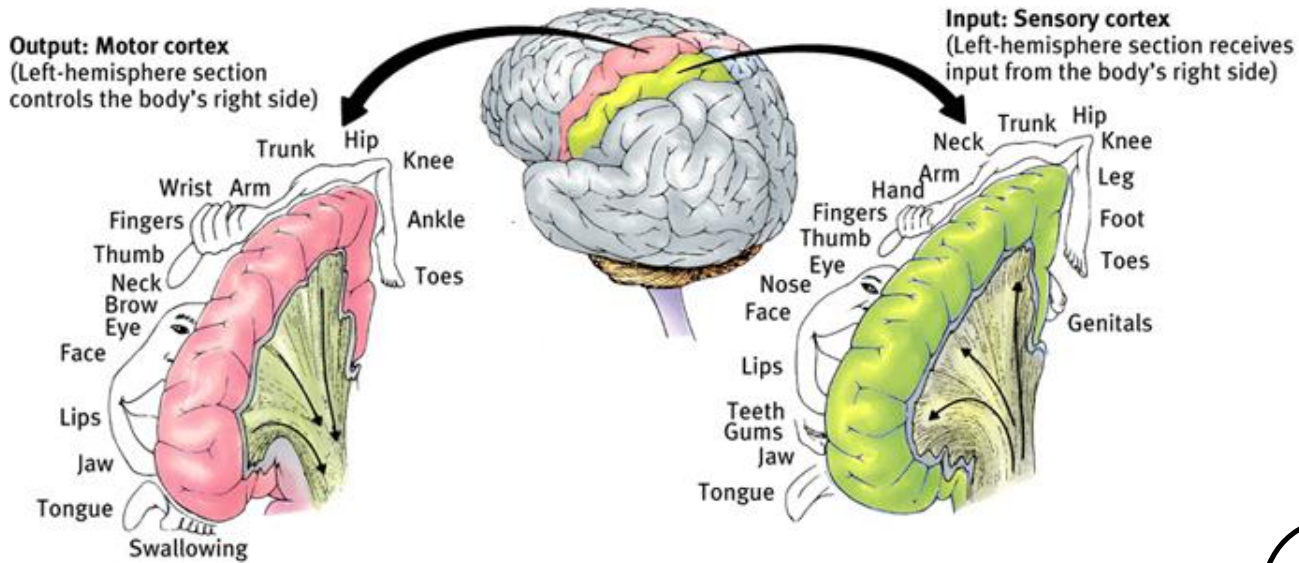


4. Example of Medical Application - Transcranial Magnetic Stimulation -

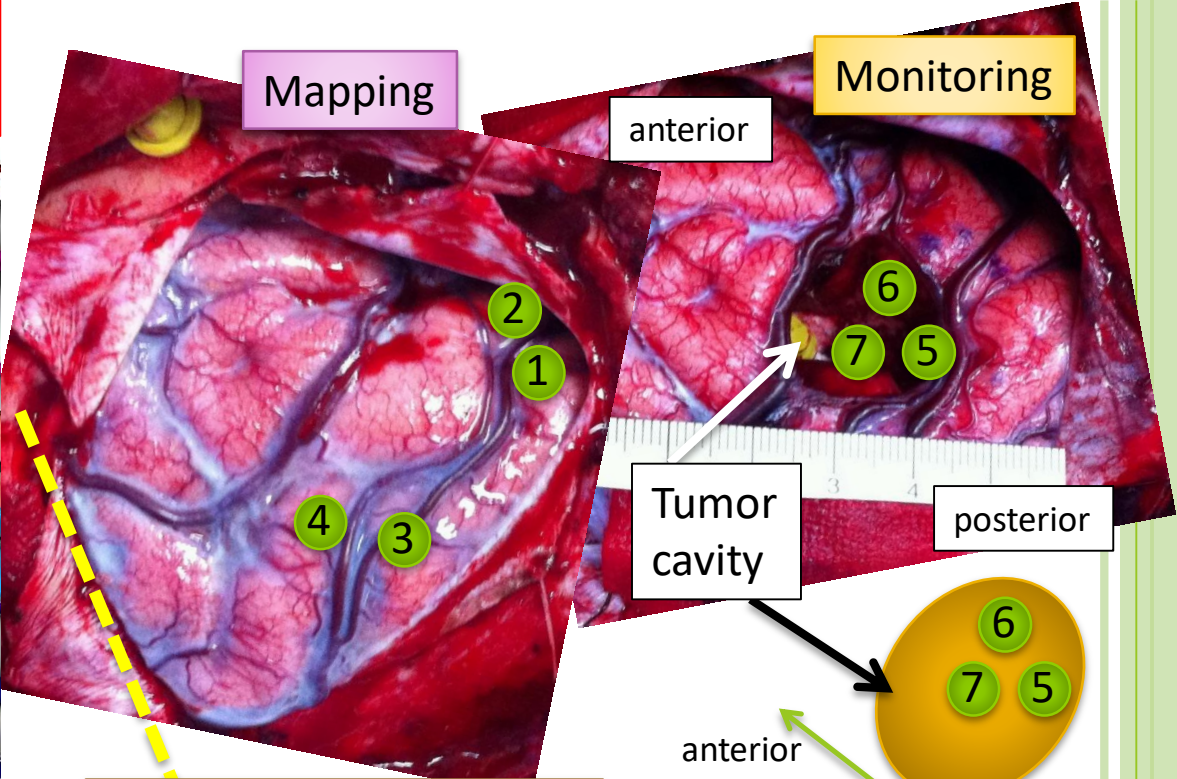
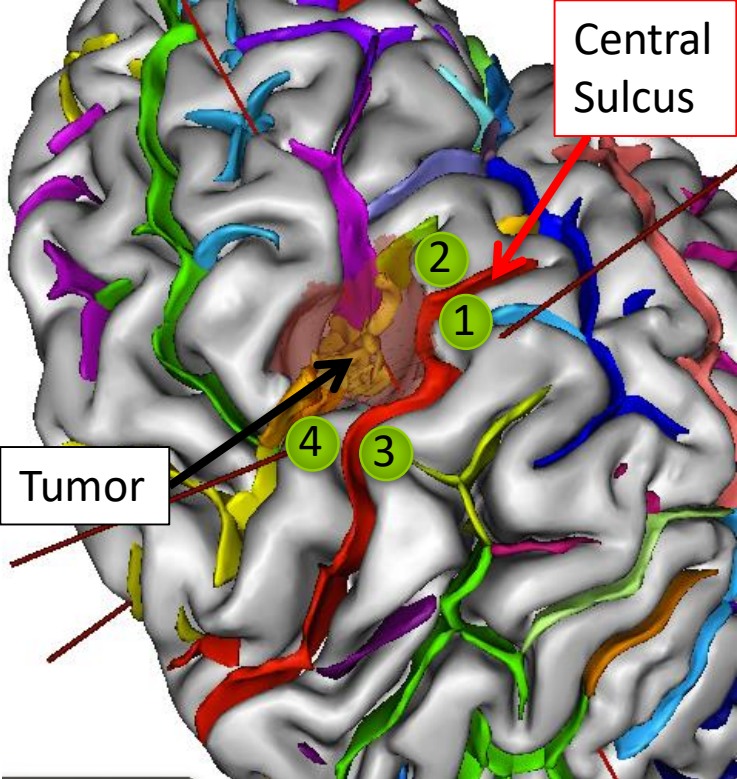
TMS IN NEUROSURGERY (1)



TMS IN NEUROSURGERY (2)



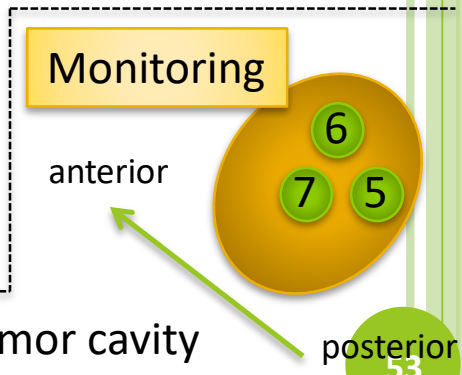
MEP: Motor evoked potential



Mapping

Motor and sensory response induced by electric stimulation (Current by Ojemann stimulator)

- ① Tongue numbness (3,6mA-positive)
- ② Left lip (orofacial) motor response (3,6mA-positive)
- ③ Left fingers numbness (3mA-negative, 6mA-positive)
- ④ **Left wrist motor response (3mA-negative, 6mA-positive)**



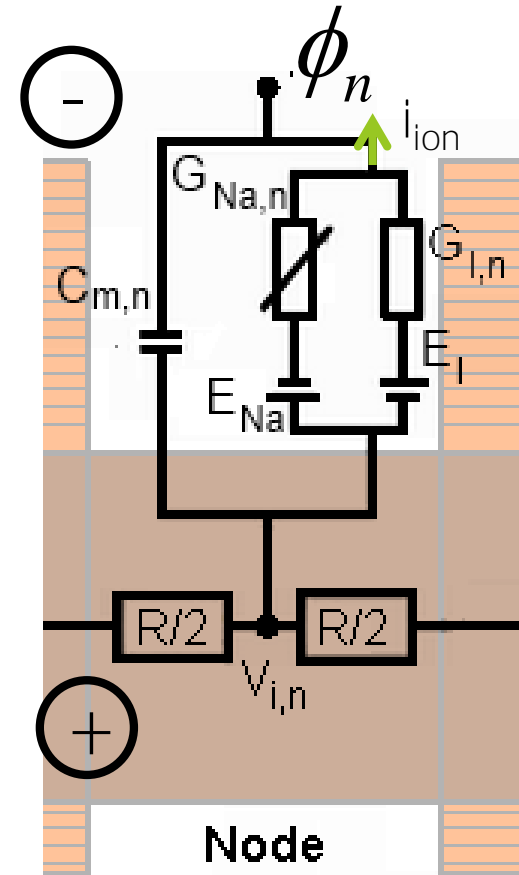
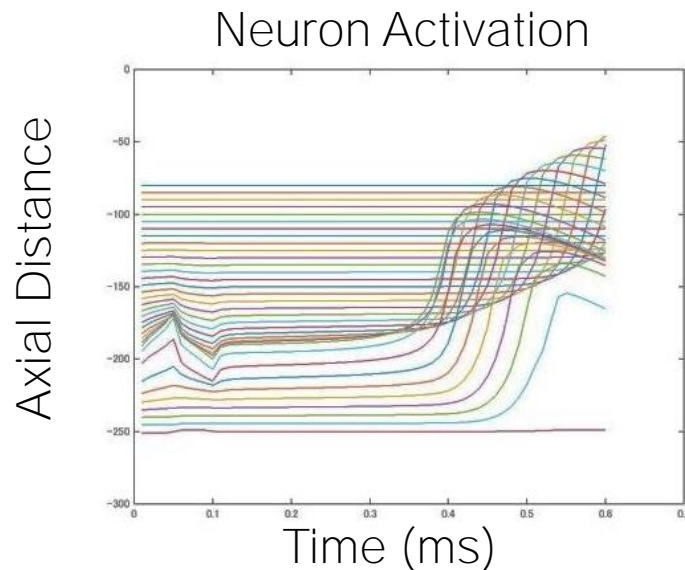
- ⑤ Left wrist (3,6mA) on tumor cavity
- ⑥ Left orofacial (1-3mA) on tumor cavity
- ⑦ Left wrist (1,3mA) on tumor cavity

Method

Detailed Model • Volume Conductor • Corticospinal Neuron

External Stimulation and Neuron

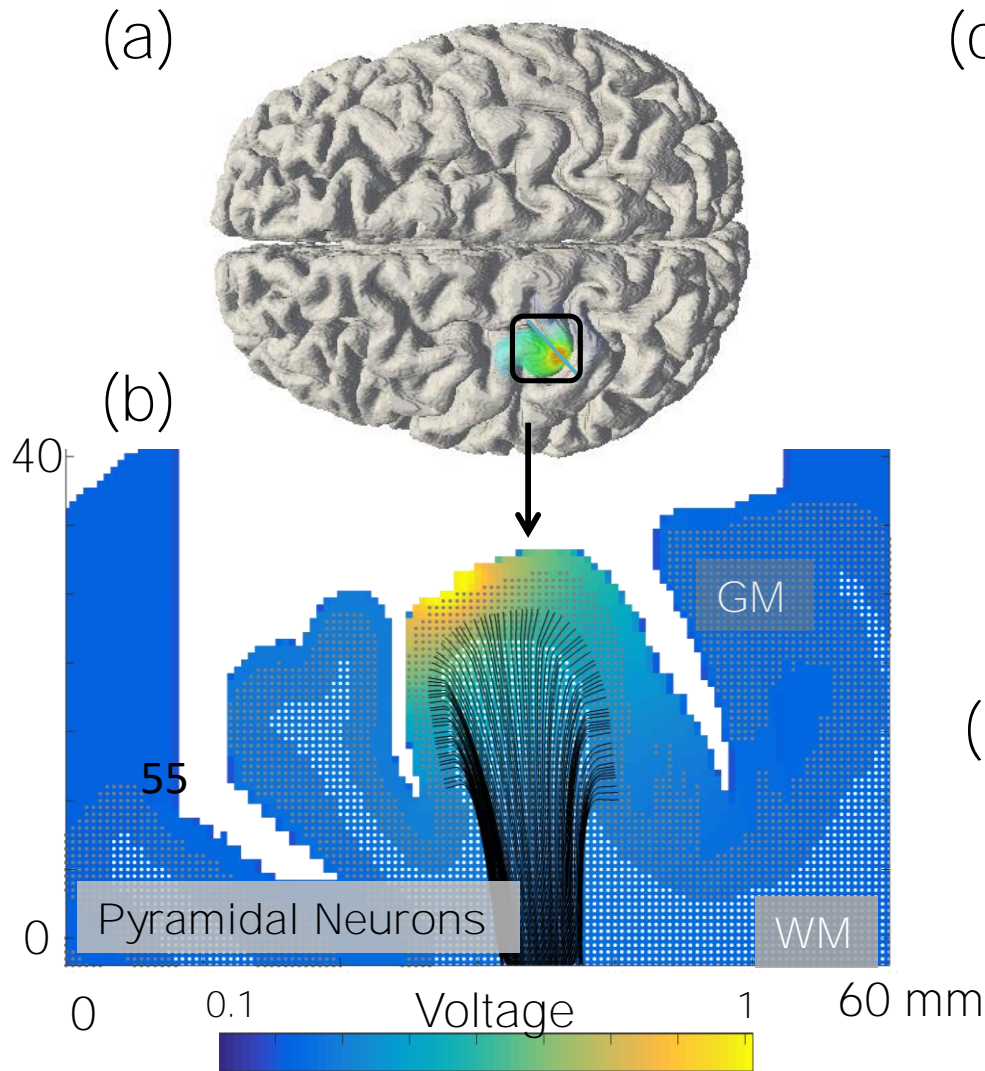
$$C_m \frac{\partial V_{m,n}}{\partial t} + \sum_x g_x (V_m - V_x) - \frac{\Delta^2 V_{m,n}}{R} = \frac{\Delta^2 \phi_n}{R}$$



$$V_{m,n} = \phi_n - \phi_{i,n}$$

Method

Detailed Model • Volume Conductor • **Corticospinal Neuron**

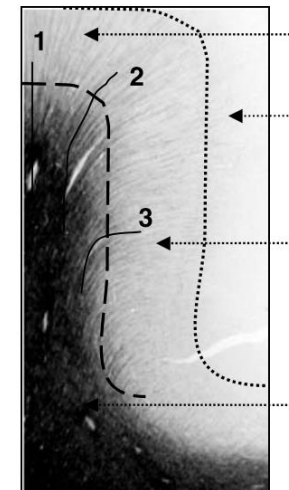


(c) 150 X 50 = 7500 neurons



— Selected Path
— Transverse Plane

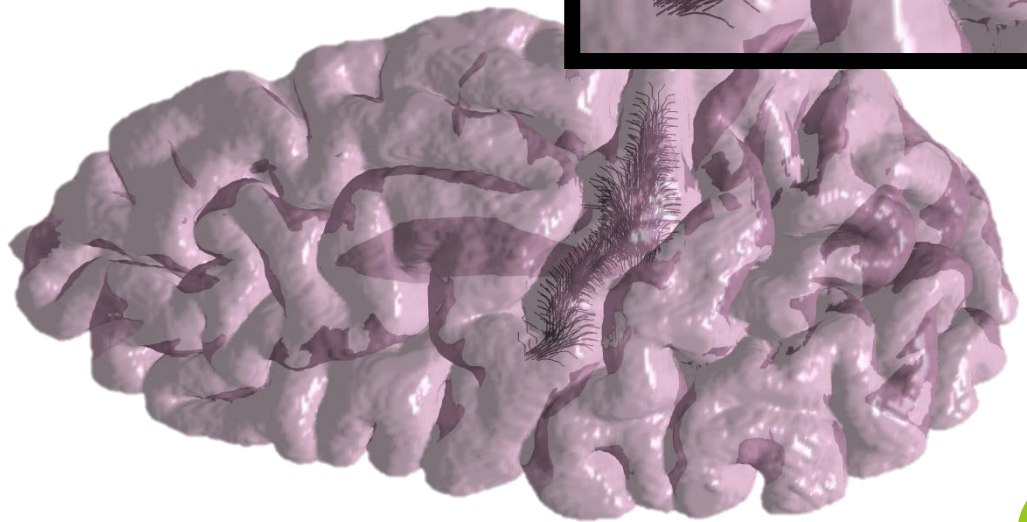
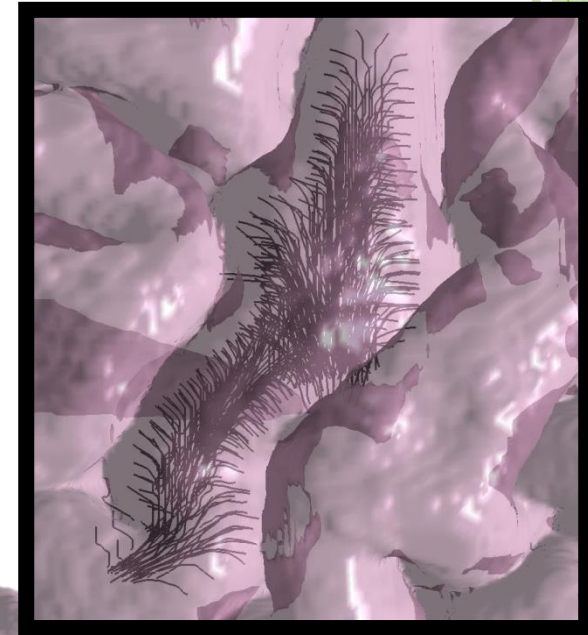
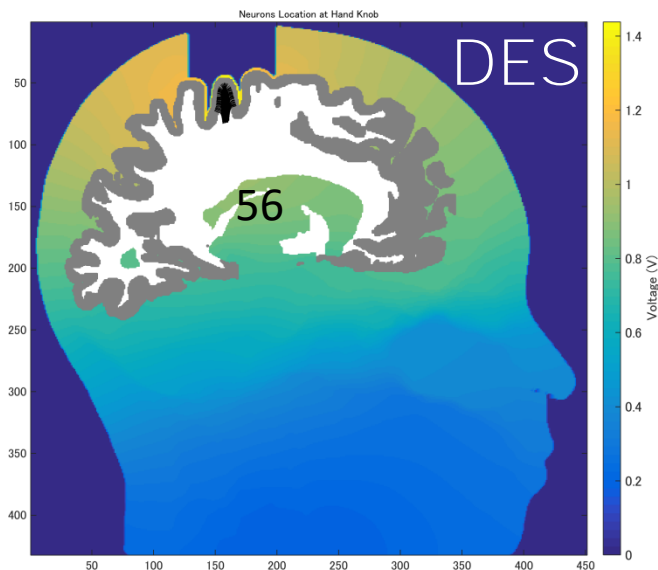
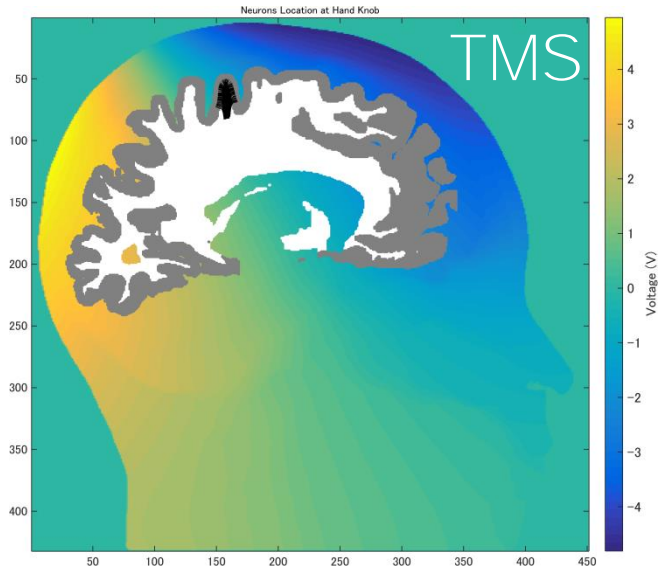
(d)



GM: Gray Matter; WM: White Matter

Method

Detailed Model • Volume Conductor • **Corticospinal Neuron**

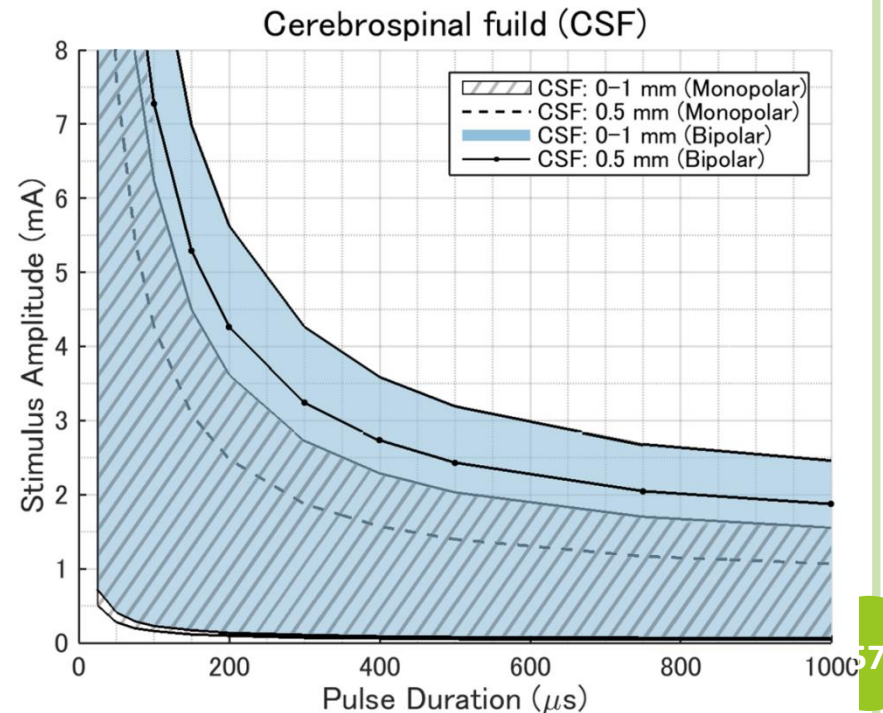
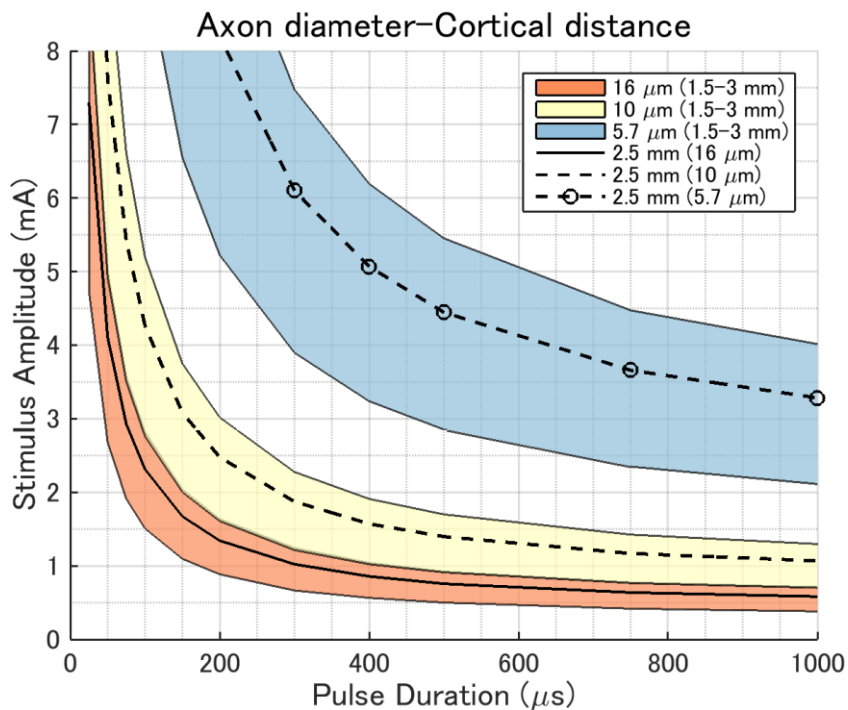


7500 neurons

Results

Nerve Parameter • E-Field • Nerve Activation

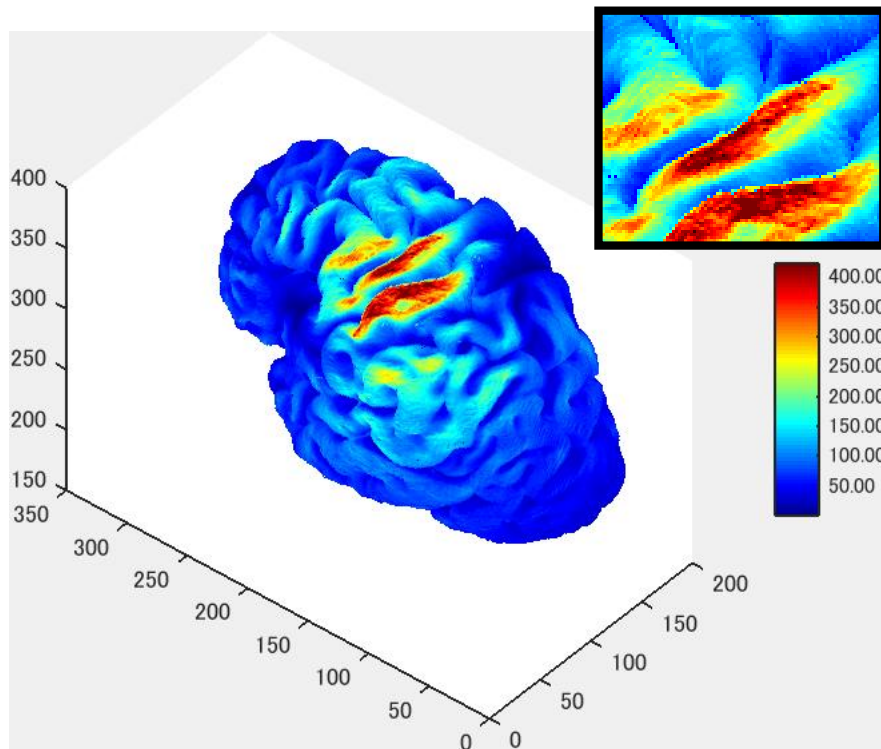
- ❑ Nerve Model Implementation/Verification
- ❑ Multiscale Simulations: Head Model + Pyramidal Neurons
- ❑ Distance: 2.5 mm from cortical surface
- ❑ Thickness: 10 μm
- ❑ CSF thickness (DES): 0.5 mm



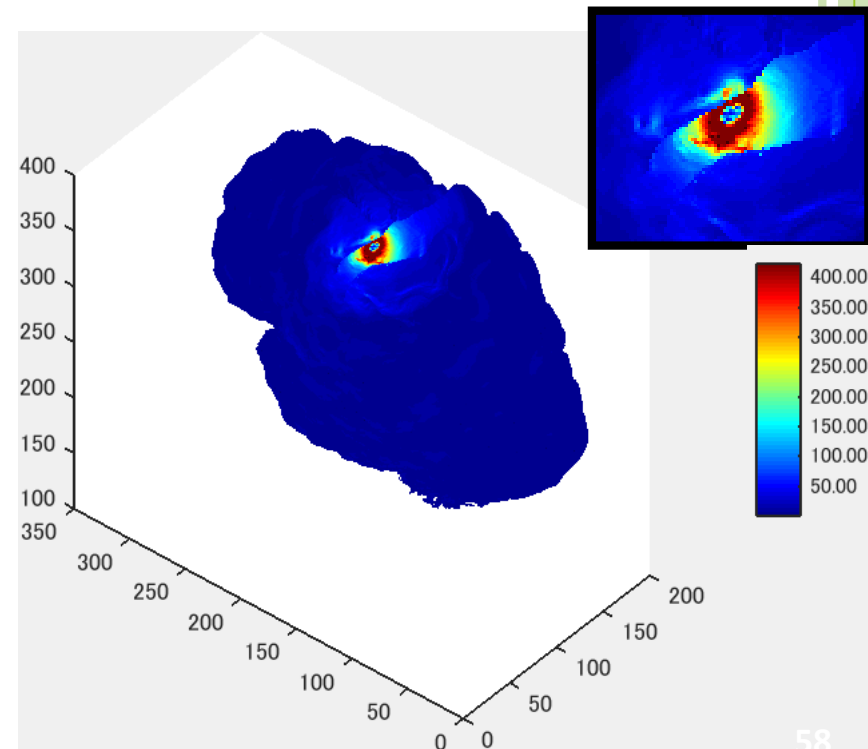
Results

Nerve Parameter • **E-Field** • Nerve Activation

- TMS coil location elicited the largest MEPs from the right FDI muscle.
- **Coil location by offline reconstruction** (geodesic distances from anatomical landmarks)
- Coil current selected to match field measurements (Nieminen et al, 2015).
- DES electrode current is 11 mA
- DES electrode position is chosen so that hotspot is similar to TMS



TMS

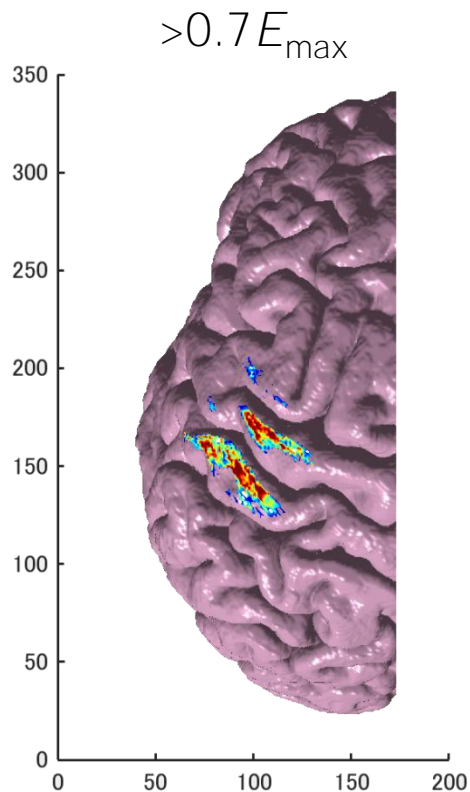


DES

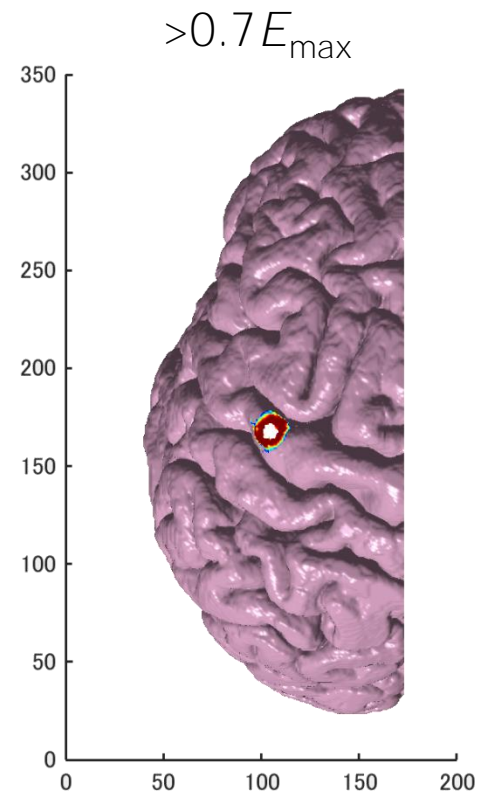
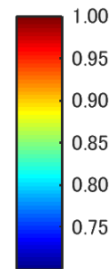
Results

Nerve Parameter • **E-Field** • Nerve Activation

- E-field concentration in the gyral crown
- E-field in TMS has a more longitudinal distribution.
- E-field in DES is around the electrode



TMS

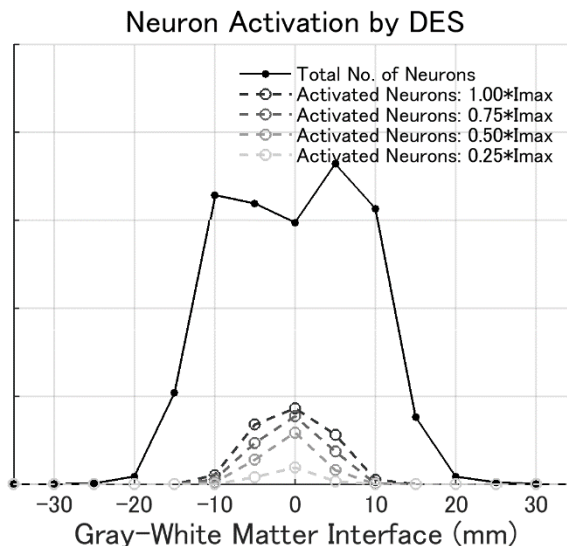
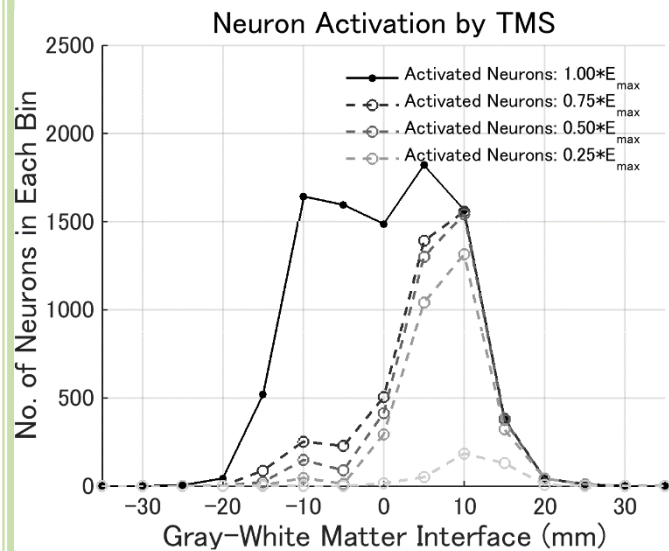


DES

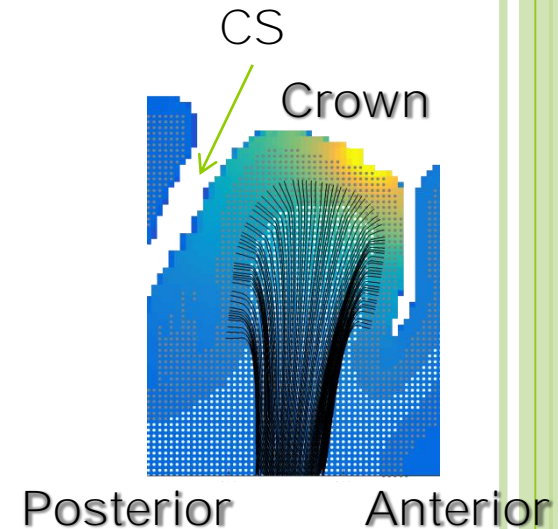
Results

Nerve Parameter • E-Field • Nerve Activation

- Neurons are grouped in bins of 5 mm.
- More nerves are activated under TMS than DES for same E_{\max}
- TMS activated nerves in the posterior wall
- DES activates nerves in the gyral crown.



Anterior Wall Crown Posterior Wall



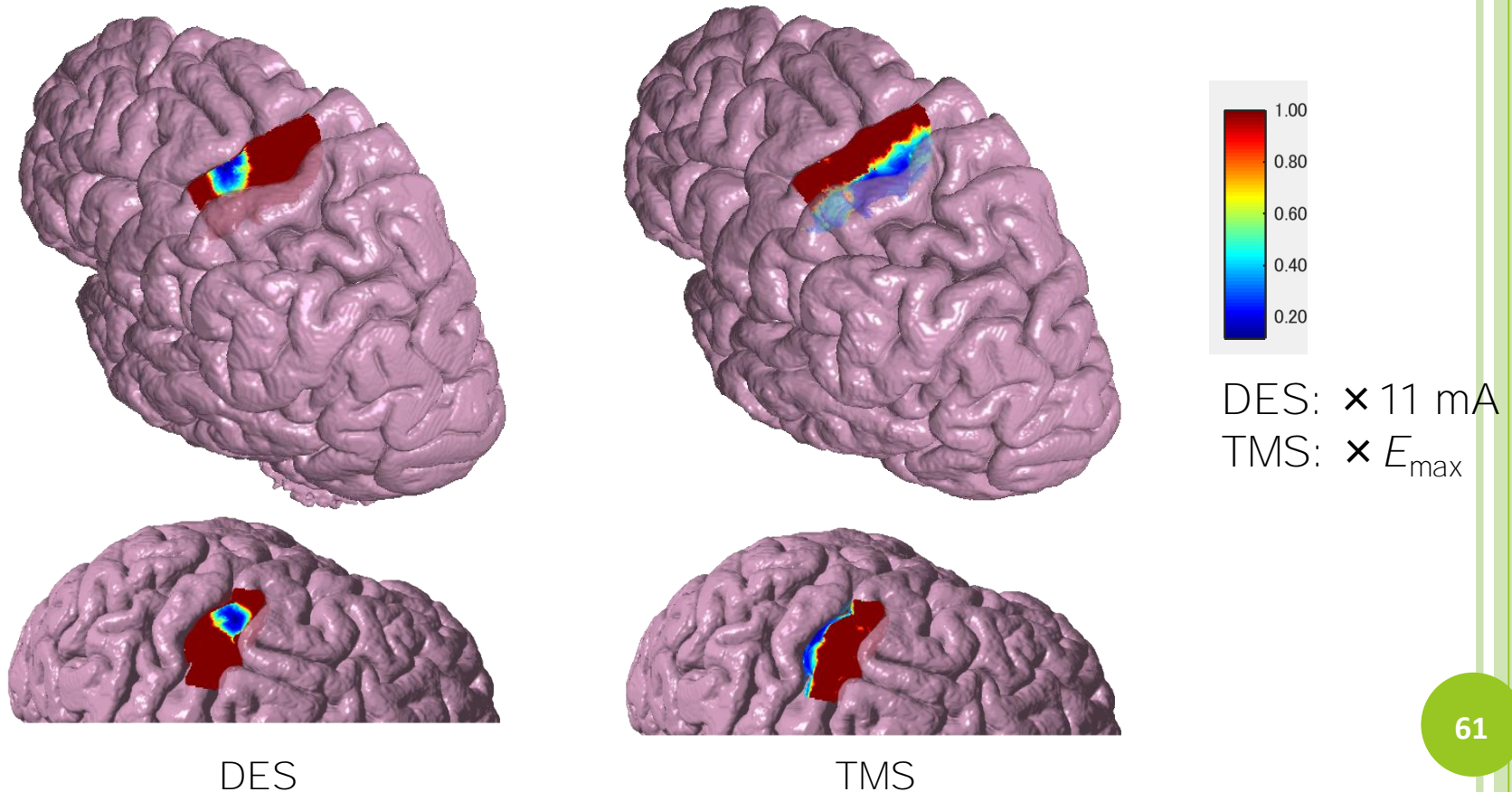
CS: Central Sulcus

✘ x-axis is the distance from the crown center

Results

Nerve Parameter • E-Field • Nerve Activation

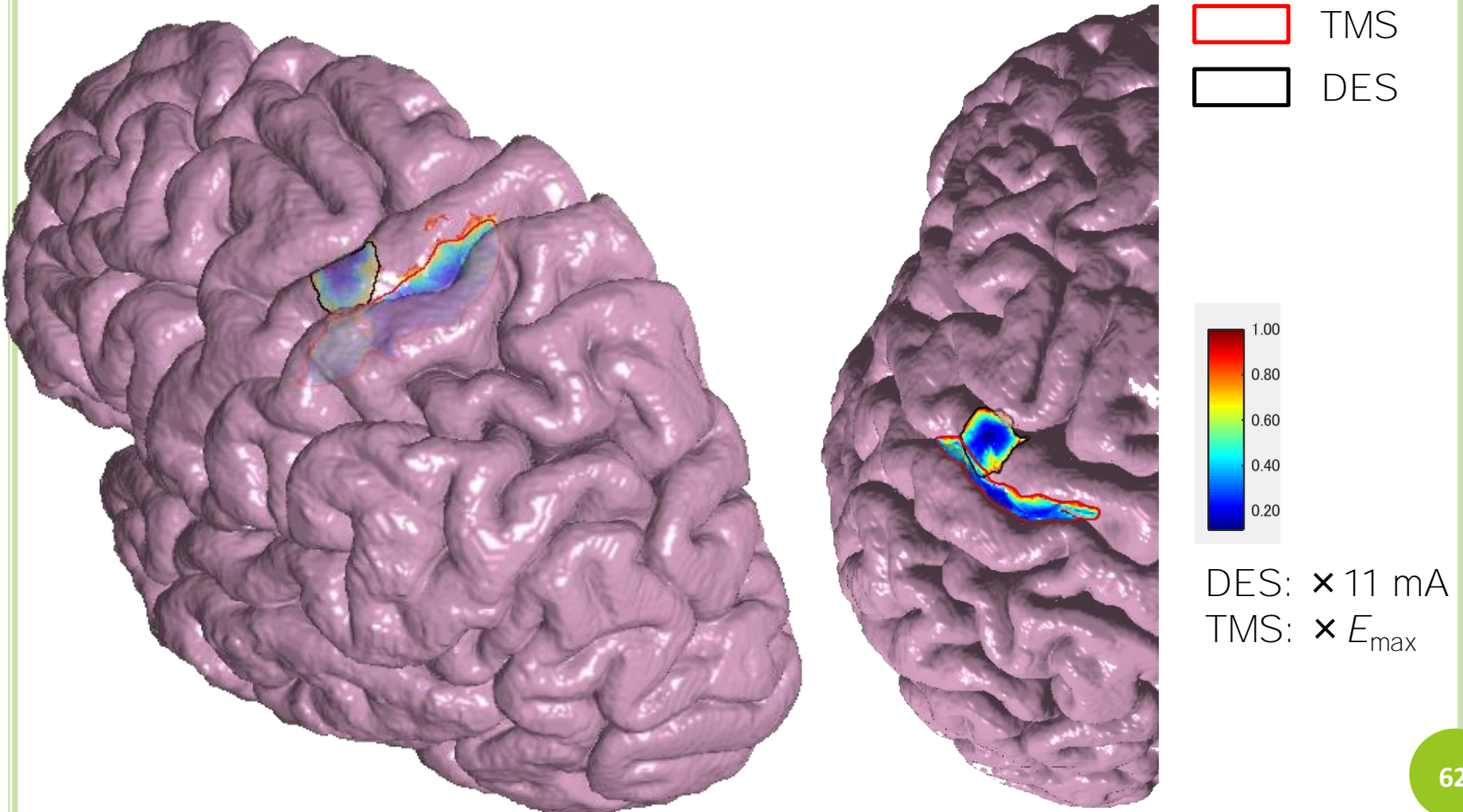
- DES: prominent mapping at precentral gyral crown
- TMS: prominent mapping at precentral sulcal wall
- TMS: axonal bends creates strong local field gradient maxima
- TMS: no focal



Results

Nerve Parameter • E-Field • Nerve Activation

- Cortical Areas Intersection (90% of $I_{\text{electrode}}$ and $I_{\text{electrode}}$)



SUMMARY

- Computational techniques are essential to evaluate the induced physical quantities in the human body models.
- International standardization bodies for human safety develop guidelines using computational data.
- Dosimetric techniques are useful even for product safety (e.g., handset antenna, new emerging techniques).
- Highly accurate computational methods are also useful for planning in medical applications.